We are IntechOpen,
the world's leading publisher of
Open Access books
Built by scientists, for scientists

6,900
Open access books available

186,000
International authors and editors

200M
Downloads

Our authors are among the

154
Countries delivered to

TOP 1%
most cited scientists

12.2%
Contributors from top 500 universities

CLARIVATE ANALYTICS
BOOK CITATION INDEX
INDEXED

WEB OF SCIENCE™

Selection of our books indexed in the Book Citation Index
in Web of Science™ Core Collection (BKCI)

Interested in publishing with us?
Contact book.department@intechopen.com

Direct Imaging of Extra-Solar Planets – Homogeneous Comparison of Detected Planets and Candidates

Ralph Neuhäuser and Tobias Schmidt
Astrophysical Institute and University Observatory,
Friedrich Schiller University Jena, Jena
Germany

1. Introduction

Planets orbiting stars other than the Sun are called *extra-solar planets* or *exo-planets*. Since about 1989, several hundred such objects were detected using various techniques. The first companions with planetary masses orbiting another star were found around a pulsar, a fast rotating neutron star, by variations of the otherwise very stable radio pulses (Wolszczan & Frail, 1992). With the radial velocity technique, one can detect the motion of the star in radial direction towards and away from us due to the fact that both a star and a planet orbit their common center of mass (first successfully done on HD 114762 and 51 Peg, Latham et al. (1989) and Mayor & Queloz (1995), respectively). This one-dimensional technique yields the lower mass limit $m \cdot \sin i$ of the companion mass m due to the unknown orbit inclination i, so that planets detected only by the radial velocity method are *planet candidates*, they could also be higher mass brown dwarfs or low-mass stars. Several hundred planet candidates were detected with this method. The reflex motion of the star in the two other dimensions due to the orbiting companion can be measured with the astrometry method (e.g. Benedict et al. (2002)), but no new planets were found with this technique so far. If the orbital plane of a planet is in the line of sight towards the Earth, then the planet will move in front of the star once per orbital period, which can be observed as transit, i.e. as small drop in the brightness of the star. This determines the inclination i and, for radial velocity planet candidates, can confirm candidates to be true planets. The transit method could confirm almost one dozen planet candidates previously detected by the radial velocity method (the first was HD 209458 b, Charbonneau et al. (2000)); in addition, more than 100 planets were originally discovered as candidates by the transit method and then confirmed by radial velocity. All the techniques mentioned above are *in*direct techniques, i.e. they all observe only the star, but not the planet or planet candidate, i.e. it is never known which photons were emitted by the star (most) and which by the planets (negligibly few). This is different only in the direct imaging technique, which we discuss below in detail. For number of planets, lists, properties, and references, see Schneider et al. (2011) with updates on www.exoplanet.eu or Wright et al. (2011) with updates on www.exoplanets.org.

For all techniques, it is also relevant to define what is called a *planet*. In the case of extra-solar planet, what is relevant is to define the upper mass limit of planets and the distinction from

brown dwarfs. For the Solar System, the International Astronomical Union (IAU) has defined the lower mass limit for planets: *A celestial body that (a) is in orbit around the Sun, (b) has sufficient mass for its self-gravity to overcome rigid body forces, so that it assumes a hydrostatic equilibrium (nearly round) shape, and (c) has cleared the neighbourhood around its orbit* (www.iau.org).

For the upper mass limit of planets, there are still several suggestions:

- The IAU *Working Group on Extrasolar Planets* has agreed on the following preliminary working definition: *Objects with true masses below the limiting mass for thermonuclear fusion of deuterium (currently calculated to be 13 Jupiter masses for objects of solar metallicity) that orbit stars or stellar remnants are planets (no matter how they formed). The minimum mass/size required for an extra-solar object to be considered a planet should be the same as that used in our Solar System. Sub-stellar objects with true masses above the limiting mass for thermonuclear fusion of deuterium are brown dwarfs, no matter how they formed nor where they are located. Free-floating objects in young star clusters with masses below the limiting mass for thermonuclear fusion of deuterium are not planets, but are sub-brown dwarfs* (www.iau.org).

- The mass (or $m \cdot \sin i$) distribution of sub-stellar companions is bi-modal, which may indicate that the two populations formed differently; the dividing mass can be used to define planets as those below the so-called *brown dwarf desert*, which lies at around ~ 25 M$_{\text{Jup}}$ (Grether & Lineweaver, 2006; Sahlmann et al., 2010; Schneider et al., 2011; Udry, 2010); Schneider et al. (2011) in their catalog on www.exoplanet.eu now include all those companions with mass below ~ 25 M$_{\text{Jup}}$ within a $1\,\sigma$ error.

- One can try to distinuish between planets and brown dwarfs by formation, e.g. that planets are those formed in circumstellar disks with solid or fluid cores and brown dwarfs being those formed star-like by direct gravitational contraction. In such a case, the mass ranges may overlap.

There is still no consensus on the definition of planets and their upper mass limit. The second and third suggestions above, however, may be consistent with each other, because the bi-modal distribution in masses may just be a consequence of different formation mechanism. We will use ~ 25 M$_{\text{Jup}}$ within a $1\,\sigma$ error as upper mass limit for this paper.

For a direct detection of a planet close to its host star, one has to overcome the large dynamical range problem (see Fig. 1 and 4): The planet is much fainter than its host star and very close to its bright host star. Normal Jupiter-like planets around low-mass stars (~ 0.1 M$_\odot$) with one to few Gyr age are 6 orders of magnitude fainter than their host stars (Burrows et al., 1997) - unless the planet would have a large albedo and would be very close to the star and, hence, would reflect a significant amount of star light, but then it is too close to the star for direct detection. Another exception are young planets, which are self-luminous due to ongoing contraction and maybe accretion, so that they are only 2 to 4 orders of magnitude fainter (for 13 to 1 Jup mass planets, respectively) than their (young) host stars, again for 0.1 M$_\odot$ stars (Burrows et al. (1997),Baraffe et al. (1998)). Hence, direct imaging of planets is less difficult around young stars with ages up to a few hundred Myr.

In this article, we will compile the planets and candidates imaged directly so far: We will compile all their relevant properties to compare them in a homogeneous way, i.e. to estimate their luminosities, temperatures, and masses homogeneously. So far, the different teams, who have found and published the objects, use different methods to estimate the companion mass,

which is the most critical parameter to decide about the nature of the object as either a planet or a brown dwarf. We will then also discuss each object individually.

2. Adaptive Optics observations to detect candidates

Given the problem of dynamical range mentioned above, i.e. that planets are much fainter than stars and very close to stars, one has to use Adaptive Optics (AO) imaging in the near-infrared JHKL bands (1 to 3.5 μm), in order to directly detect a planet, i.e. to resolve it from the star. The infrared (IR) is best, because planets are cool and therefore brightest in the near- to mid-IR, while normal stars are brighter in the optical than in the IR. Two example images are given in Fig. 1.

Before any planets or planet candidates became detectable by ground-based AO observations, brown dwarfs as companions to normal stars were detected, because brown dwarfs are more massive and, hence, brighter, Gl 229 B being the first one (Nakajima et al. (1995), Oppenheimer et al. (1995)).

We will now present briefly the different observational techniques.

In *normal near-IR imaging* observations, even without AO, one would also take many short exposures in order not to saturate the bright host star (typically on the order of one second), with some offset either after each image or after about one minute (the time-scale after which the Earth atmosphere changes significantly) - called jitter or dither pattern. One can then subtract each image from the next or previous image (or a median of recent images) in order to subtract the background, which is actually foreground emission from Earth atmosphere etc. Then, one can add up or median all images, a procedure called shift+add. Without AO and/or with exposure times much longer than the correlation time of the atmosphere, such images will be far from the diffraction limit. Objects like TWA 5 B (Fig. 1) or HR 7329 B, also discussed below, were detected by this normal IR imaging with the 3.5m ESO NTT/SofI (Neuhäuser, Guenther, Petr, Brandner, Huélamo & Alves (2000),Guenther et al. (2001)).

In *speckle imaging*, also without AO, each single exposure should be as short as the correlation time of the atmosphere (at the given wavelength), so that each image can be diffraction-limited. Then, one also applies the shift+add technique. A faint planet candidate near TWA 7 was detected in this way with the 3.5m ESO NTT/Sharp (Neuhäuser, Brandner, Eckart, Guenther, Alves, Ott, Huélamo & Fernández, 2000), but later rejected by spectroscopy (Neuhäuser et al., 2002).

In *Adaptive Optics* (AO) IR imaging, each single exposure should also be short enough, in order not to saturate on the bright host star. If the host star image would be saturated, one cannot measure well the position of the photocenter of its PSF, so that the astrometric precision for the common proper motion test would be low. One also applies the shift+add technique. Most planets and candidates imaged directly were detected by normal AO imaging, see e.g. Fig. 1 (TWA 5), but are also limited regarding the so-called *inner working angle*, i.e. the lowest possible separation (e.g. the diffraction limit), at which a faint planet can be detected. The diffraction limit ($\sim \lambda/D$) at D=8 to 10 meter telescopes in the K-band ($\lambda = 2.2\,\mu$m) is 0.045 to 0.057 arc sec; one cannot improve the image quality (i.e. obtain a smaller diffraction limit) by always increasing the telescope size because of the seeing, the turbulence in the Earth atmosphere, hence AO corrections. One can combine the advantages of speckle and AO, if the

individual exposures are very short and if one then saves all exposures (so-called *cube mode* at ESO VLT NACO AO instrument).

If the host star nor any other star nearby (in the isoplanatic patch) is bright enough as AO guide star, then one can use a *Laser Guide Star*, as e.g. in the Keck AO observations of Wolf 940 A and B, a planet candidate (Burningham et al., 2009), see below.

One can also place the bright host star behind a coronagraph, so that the magnitude limit will be larger, i.e. fainter companions would be detectable. However, one then cannot measure the photocenter position of the host star, so that the astrometric precision for the common proper motion test would be low. One can use a *semi-transparent coronagraph*, so that both star and companion are detected. We show an example in Fig. 1, the star ϵ Eri, where one close-in planet may have been detected by radial velocity and/or astrometry (Hatzes et al. (2000),Benedict et al. (2006)) and where there are also asymmetries in the circumstellar debris disk, which could be due to a much wider planet; such a wide planet might be detectable with AO imaging, but is not yet detected - neither in Janson et al. (2007) nor in our even deeper imaging observation shown in Fig. 1.

For any AO images with simple imaging (shift+add), or also when using a semi-transparent coronagraph and/or a Laser Guide Star, one can then also subtract the Point Spread Function (PSF) of the bright host star after the shift+add procedure, in order to improve the dynamic range, i.e. to improve the detection capability for very small separations (see Fig. 4). For *PSF subtraction*, one can either use another similar nearby star observed just before or after the target (as done e.g. in the detection of β Pic b, Lagrange et al. (2009)) or one can measure the actual PSF of the host star in the shift+add image and then subtract it.

Moreover one can obtain the very highest angular resolutions at the diffraction limit by using sparse aperture interferometric masks in addition to AO. While very good dynamic ranges can be achieved very close to stars, the size of the apertures in masking interferometry is limited by the number of holes which are needed, in order to preserve non-redundancy, thus limiting the total reachable dynamic range. Currently reached detection limits at VLT can be found e.g. in Lacour et al. (2011), beginning to reach the upper mass limits for planets given above.

In order to reduce present quasistatic PSF noise further one can use another technique called Angular Differential Imaging (ADI) (Marois et al., 2006). Using this method a sequence of images is acquired with an altitude/azimuth telescope, while the instrument field derotator is switched off, being the reason for the technique's alias name Pupil Tracking (PT). This keeps the instrument and telescope optics aligned and allows the field of view to rotate with respect to the instrument. For each image, a reference PSF is constructed from other appropriately selected images of the same sequence and subtracted before all residual images are then rotated to align the field and are combined.

This technique was further improved by introducing an improved algorithm for PSF subtraction in combination with the ADI. Lafrenière, Marois, Doyon, Nadeau & Artigau (2007) present this new algorithm called 'locally optimized combination of images' (LOCI).

While the ADI is inefficient at small angular separations, the simultaneous Spectral Differential Imaging (SDI) technique offers a high efficiency at all angular separations. It consists in the simultaneous acquisition of images in adjacent narrow spectral bands within a spectral range where the stellar and planetary spectra differ appreciably (see Lafrenière, Doyon, Nadeau, Artigau, Marois & Beaulieu, 2007, and references therein).
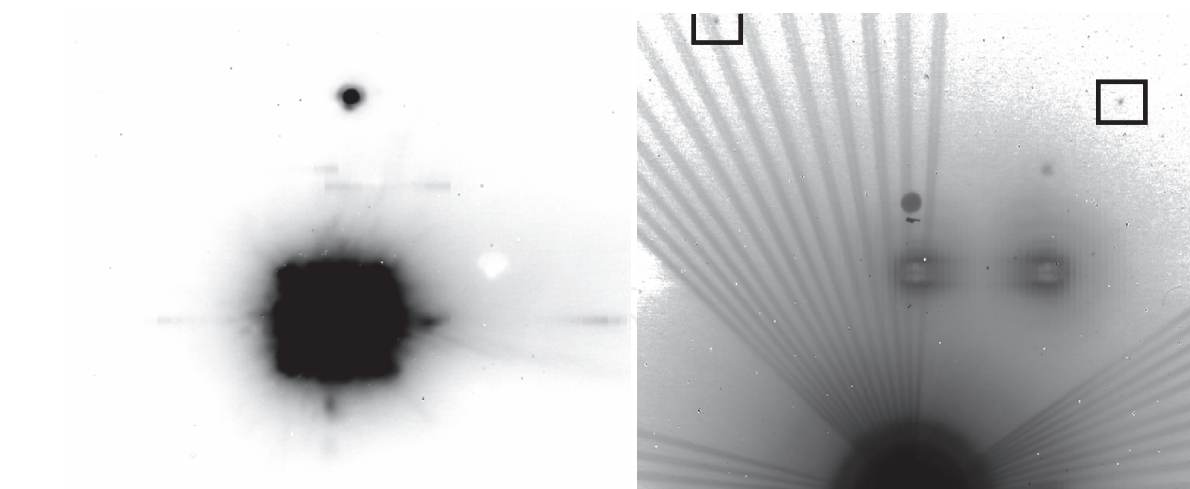
Fig. 1. Left: Our latest AO image of TWA 5 A (center) and B (2 arc sec north of A) obtained with VLT/NACO on 2008 June 13 in the K band. The mass of the companion is in the range of 17 to 45 M_{Jup} according to the Burrows et al. (1997) model (Table 2). Right: Our recent AO image of ϵ Eri obtained with VLT/NACO with the star located behind a semi-transparent coronagraph. Due to the large brightness of the star, reflection effects are also strong. Several very faint objects are detected around ϵ Eri (see boxes); however, they are all non-moving background objects as found after two epochs of observations; there is no planet nor planet candidate detected, yet, nor any additional faint object with only one epoch of imaging observation. Asymmetries in the debris disk around ϵ Eri might be due to a wide planet.

Moreover different kinds of phase masks are in use and are especially effective in combination with Adaptive Optics and a coronagraph. Recently Quanz et al. (2010) presented first scientific results using the Apodizing Phase Plate coronagraph (APP) on VLT NACO to detect β Pic b at 4 μm.

One can also detect planets as companions to normal stars with optical imaging from a *space telescope* like the Hubbe Space Telescope, see e.g. Kalas et al. (2008) for the images of the planet Fomalhaut b. From outside the Earth atmosphere, there is no atmospheric seeing, so that one can always reach the diffraction limit.

Previous reviews of AO imaging of planets were published in Duchêne (2008), Oppenheimer & Hinkley (2009), and Absil & Mawet (2010). Previous homogeneous mass determinations of planets and candidates imaged directly were given in Neuhäuser (2008) and Schmidt et al. (2009).

3. Proper motion confirmation of candidates

Once a faint object is directly detected close to a star, one can consider it a planet *candidate*, which needs to be confirmed. Two common tests can be performed on such candidates:
(a) Common proper motion test: Both the star and the planet have to show the same (or at least very similar) proper motion. The host star is normally a relatively nearby star (up to a few hundred pc, otherwise the planet would be too faint, i.e. not detectable), so that its proper motion is normally known. If the faint object would be a background star, it would be 1 to several kpc distant, so that its proper motion should be negligible compared to the star. Hence, if both the star and the faint object show the same proper motion, then the companion is not

a non-moving background star, but a co-moving companion. Given the orbital motion of the star and its companion, depending on the inclination and eccentricity, one would of course expect that their proper motions are not identical, but the differences (typically few milli arc sec per year, mas/yr) are negligible compared to the typical proper motions. Instead of (or best in addition to) common proper motion, it is also sufficient to show that both objects (primary and companion candidate) show the same radial velocity, and that the secular evolution of the radial velocity is consistent with orbital motion and inconsistent with the background hypothesis.

(b) Spectrum: If the faint object next to the star would be a planet, its mass and temperature should be much smaller than for the star. This can be shown by a spectrum. Once a spectrum is available, one can determine the spectral type and temperature of the companion. If those values are consistent with planetary masses, then the faint object is most certainly a planet orbiting that star. However, it could still be a very low-mass cool background object (very low-mass L-type star or L- or T-type brown dwarf). In cases where the companion is too faint and/or too close to the star, a spectrum might not be possible, yet, so that one should try to detect the companion in different bands to measure color indices, which can also yield (less precise) temperature or spectral type; then, however, one has the problem to distinguish between a reddened background object and the truly red (i.e. cool, e.g. planetary) companion.

The case of the ScoPMS 214 companion candidate (no. 1 or B) has shown that both tests are neccessary for a convincing case: The young K2 T Tauri star ScoPMS 214, member of the Scorpius T association, shares apparently common proper motion with a faint object nearby (3 arc sec separation) over five years; however, a spectrum of this companion candidate has shown that it is a foreground M dwarf (Metchev & Hillenbrand, 2009). Hence, the spectroscopic test is indeed necessary. Also, red colors alone (even if together with common proper motion) is not convincing, because a faint object near a star could just be reddened by extinction (background) instead of being intrinsically red, i.e. cool.

It is not sufficient to show that a star and a faint object nearby show the same proper motion (or proper motion consistent within 1 to 3 σ), one also has to show that the data are inconsistent with the background hypothesis. Common proper motion can be shown with two imaging detections with an epoch difference large enough to significantly reject the background hypothesis, namely that the faint object would be an unrelated non-moving background object. The epoch difference needed depends on the astrometric precision of the detector(s) used and the proper motion of the host star. We show an example in Fig. 2 and 3. Spectra are usually taken with an infrared spectrograph with a large telescope and AO.

Fig. 2 shows the change in separation between TWA 5 A and B with time, Fig. 3 shows the position angle (PA) of TWA 5 B with respect to TWA 5 A. In Fig. 3, the expectation for the background hypothesis is also plotted and clearly rejected by many σ. All data points are consistent with TWA 5 A and B being a common proper motion pair. Both the PA and the separation values decrease since the first detection in 1999. Such a (small) change in separation and/or PA can be interpreted as evidence of orbital motion, which of course has to be expected. One can conclude from these data that the orbit is eccentric and/or inclined.

A detection of a change in either separation or PA is actually a detection of a difference in the proper motions of A and B. It can be interpreted as evidence for slightly different proper motion. Given that most directly imaged planets (or candidates) are detected close
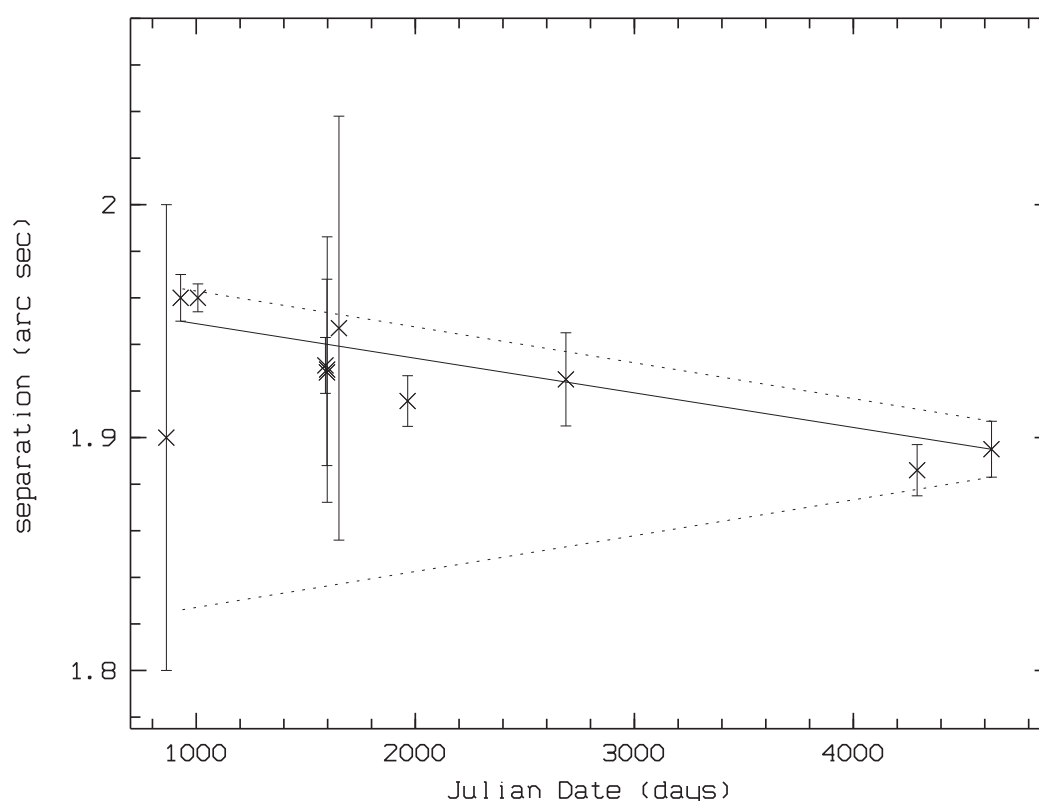
Fig. 2. Separation (in arc sec) versus observing epoch (JD - 2450000 in days) between the host star TWA 5 A (actually the photo-center of close Aa+B pair) and the sub-stellar companion TWA 5 B using data from Neuhäuser et al. (2010). The dotted lines (starting from the 2008 data point opening to the past) indicate maximum possible separation change due to orbital motion for a circular edge-on orbit. The expectation for the background hypothesis is not shown for clarity (and is rejected in Fig. 3). All data points are fully consistent with common proper motion, but not exactly identical proper motion (constant separation). Instead, the data are fully consistent with orbital motion: The separation decreases on average by ~ 5.4 mas per year, as shown by the full line, which is the best fit. The figure is adapted from Neuhäuser et al. (2010).

to members of young associations (like TWA, Lupus, β Pic moving group etc.), it is therefore also possible that both the host star A and the faint object nearby (B or b) are both independent members of that association, not orbiting each other. Such an association is partly defined by the way that all or most members show a similar proper motion. In such cases, it might be necessary to show not only common proper motion (i.e. similar proper motion within the errors) or slightly different proper motion (consistent with orbital motion), but also curvature in the orbital motion. Such curvature would be due to acceleration (or deceleration) in case of a non-circular orbit. It could also be due to apparent acceleration (or deceleration) in the 2-dimensional apparent orbit on the plane of the sky for an orbit that is inclined towards the plane of the sky. Curvature can also be detected if the faint object is not anymore a bound
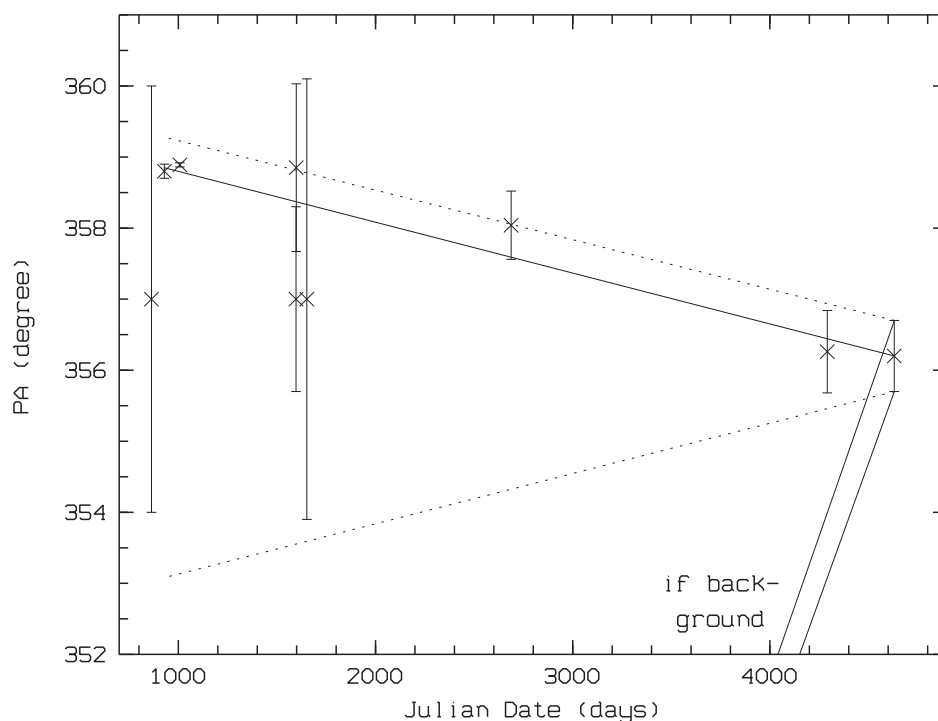
Fig. 3. Position angle PA (in degrees) versus observing epoch (JD - 2450000 in days) for TWA 5 B with respect to TWA 5 A (actually the photo-center of close Aa+B pair) using data from Neuhäuser et al. (2010). The dotted lines (starting from the 2008 data point opening to the past) indicate maximum possible PA change due to orbital motion for a circular pole-on orbit. The full lines with strong positive slope in the lower right corner are for the background hypothesis, if the bright central star (TWA 5 A) moved according to its known proper motion, while the fainter northern object (now known as B) would be a non-moving background object; the data points are inconsistent with the background hypothesis by many σ. All data points are fully consistent with common proper motion, but not exactly identical proper motion (constant PA). Instead, the data are fully consistent with orbital motion: The PA appears to decrease by $\sim 0.26°$ per year, as shown by the full line, which is the best fit. The figure is adapted from Neuhäuser et al. (2010).

companion, but is currently been ejected, i.e. on a hyperbolic orbit. Hence, to convincingly prove that a faint object is a bound companion, one has to show curvature that is not consistent with a hyperbolic orbit.

For all of the directly imaged planets and candidates listed below, common proper motion between the candidate and the host star has been shown. For only few of them, evidence for orbital motion is shown, e.g. DH Tau (Itoh et al., 2005) GQ Lup (Neuhäuser et al., 2008), Fomalhaut (Kalas et al., 2008), HR 8799 bcde (Marois et al., 2008; 2010), TWA 5 (Neuhäuser et al., 2010), PZ Tel (Mugrauer et al., 2010), β Pic (Lagrange et al., 2010), and HR 7329 (Neuhäuser et al., 2011). For only two of them, curvature in the orbital motion was detected, namely in PZ Tel (Mugrauer et al., 2010) and TWA 5 (Neuhäuser et al., 2010).

4. Data base: Planets and candidates imaged directly

Searching the literature, we found 25 stars with directly imaged planets and candidates. We add 2M1207, a planet candidate imaged directly, whose primary would be a brown dwarf. In two cases, there is more than one planet (or candidate) detected directly to orbit the star: 4 planets around HR 8799 and two candidates in the GJ 417 system, see below. Most planets and candidates orbit single stars, but there are some as members of hierachical systems with three or more objects (one planet candidate plus two or more stars, such as TWA 5 or Ross 458). We gathered photometric and spectral information for all these objects, to derived their luminosities in a homogeneous way, taking a bolometric correction into account (Table 1). According to the mass estimate in Table 2, all of them can have a mass below 25 M_{Jup}, so that they are considered as planets.

The masses of such companions can be determined in different ways, the first two of which are usually used:

- Given the direct detection of the companion, its brightness is measured. If the companionship to the star is shown, e.g. by common proper motion, then one can assume that the companion has the same distance and age as its host star. If either a spectrum or color index is also observed, one can estimate the temperature of the companion, so that the bolometric correction can be determined; if neither color nor spectrum is available, one can often roughly estimate the temperature from the brightness difference, assuming companionship. From brightness, bolometric correction, and distance, one can estimate the luminosity. Using theoretical evolutionary models, one can then estimate the mass from luminosity, temperature, and age. However, those models are uncertain due to unknown initial conditions and assumptions. In particular for the youngest systems, below 10 Myr, the values from the models are most uncertain. Masses derived in this way are listed in Table 2.

- If a good S/N spectrum with sufficient resolution is obtained, one can also measure the effective temperature and surface gravity of the companion. Then, from temperature and luminosity, one can estimate the companion radius. Then, from radius and gravity, one can estimate the companion mass. This technique is independent of the uncertain models, but needs both distance and gravity with good precision. Since gravities (and sometimes also distances) cannot be measured precisely, yet, the masses derived in this way typically have a very large possible range.

- In the case of the directly imaged planet around the star Fomalhaut, an upper mass limit of ~ 3 M_{Jup} for the companion could be determined by the fact that a dust debris ring is located just a few AU outside the companion orbit (Kalas et al., 2008). In other planet candidates also orbiting host stars with debris disks, such an upper mass limit estimate should also be possible, e.g. in HR 8799 (Marois et al. (2008),Reidemeister et al. (2009)), β Pic (see Freistetter et al., 2007), PZ Tel (Biller et al. (2010),Mugrauer et al. (2010)), and HR 7329 (Neuhäuser et al., 2011).

- If there are several planets or candidates imaged around the same star, then one can also try to determine masses or limits by stability arguments, see e.g. HR 8799 (Marois et al. (2008),Reidemeister et al. (2009)).

- If there are other sub-stellar objects with very similar values regarding temperature, luminosity, and age, for which there is also a direct mass estimate, e.g. directly obtained

in an eclipsing double-lined binary such as 2M0535 (Stassun et al., 2006) or in a visually resolved system with full orbit determination such as HD 130948 BC (Dupuy et al., 2009), one can conclude that the sub-stellar companion in question also has a similar mass. If a sub-stellar companion has temperature and luminosity smaller than another sub-stellar object with a direct mass estimate, but the same age, then the sub-stellar companion in question should have a smaller mass. For HD 130948 BC, there is only an estimate for the total mass being 114 ± 3 M$_{\mathrm{Jup}}$ (Dupuy et al., 2009), i.e. somewhat too large for comparison to planet candidates. The object 2M0535 is an eclipsing double-lined spectroscopic binary comprising of two brown dwarfs, member of the Orion star forming region, hence not older than a few Myr, maybe below 1 Myr. For a double-lined spectroscopic binary, one can determine brigtness, temperatures, luminosities, and lower mass limits $m \cdot \sin i$ for both objects individually. The orbital inclination i can then be obtained from the eclipse light curve. Hence, both masses are determined dynamically without model assumptions, the masses are 60 ± 5 M$_{\mathrm{Jup}}$ for A and 38 ± 3 M$_{\mathrm{Jup}}$ for B (Stassun et al., 2007). Given that several of the sub-stellar companions discussed here have a very similar age, we can compare them with 2M0535 A and B. If all parameters are similar, than the masses should also be similar. If a companion has lower values (at a similar age), i.e. being cooler and fainter, then it will be lower in mass. See Table 1 and 2 for the values and the comparison. Such a comparison should also be done with great care, because also other properties like magnetic field strength, spots on the surface, and chemical composition (metallicity) affect the analysis.

- If one could determine a full orbit of two objects around each other, one can then estimate the masses of both the host star and the companion using Kepler's 3rd law as generalized by Newton. However, since all planets and planet candidates imaged directly so far have large separations (≥ 8.5 AU) from their host star (otherwise, they would not have been detected directly), the orbital periods are typically tens to hundreds of years, so that full orbits are not yet observed.

5. Comments on individual objects

Here, we list data, arguments, and problems related to the classification of the companions as planets. We include those sub-stellar companions, where the common proper motion with a *stellar* primary host star has been shown with at least 3 σ and where the possibly planetary nature, i.e. very low mass and/or cool temperature, has been shown by a spectrum - or at least a very red color with known (small) extinction, in order to exclude reddened background objects. We also include the brown dwarf 2M1207 with its fainter and lower-mass sub-stellar companion, even though the primary object is not a star, but we do not list other brown dwarfs with possibly planetary mass companions. We include only those systems in our list for new and homogeneous mass determination, where the age is considered to be possibly below $\sim$ 500 Myr, otherwise age and sub-stellar companion mass is probably too large; however, we do include those older systems, where the mass of the sub-stellar companion has already been published and estimated to be near or below $\sim$ 25 M$_{\mathrm{Jup}}$, e.g. WD 0806-661 (Luhman et al., 2011) and Wolf 940 B (Burningham et al., 2009). We also exclude those systems, however, where the age is completely unconstrained, e.g. HD 3651 (Mugrauer et al., 2006), GJ 758 (Thalmann et al., 2009), and several others listed, e.g., in Faherty et al. (2010). This compilation is the 3rd version (after Neuhäuser (2008) and Schmidt et al. (2009)) and we do plan to renew and enlarge the catalog later; then, we will consider to also include possibly planetary mass

companions imaged directly around sub-stellar primaries and around old stars or stars with unconstrained age.

We list the objects in the chronologic order of the publications of the common proper motion confirmations; if the significant confirmation were published later than the discovery, we list the object at the later date.

GG Tau Bb: The T Tauri star GG Tau in the Taurus T association (hence 0.1 to 2 Myr young at ~ 140 pc distance) is a quadruple system with two close pairs GG Tau Aa+Ab (separation $\sim 0.25''\simeq 35$ AU, the fainter component in this northern binary is sometimes called GG Tau a) and GG Tau Ba+Bb ($\sim 1.48''\simeq 207$ AU), the separation between A and B is $10''$. The system has been studied in detail by White et al. (1999) using the HST as well as HIRES and LRIS at Keck. The object of interest here is GG Tau Bb, also called GG Tau/c. White et al. (1999) determine a spectral type of M7, zero extinction, Lithium absorption, and Hα emission (hence, young, not a reddened background object). According to Baraffe et al. (1998) models, at the age and distance of the star GG Tau Ba, the sub-stellar object GG Tab Bb has a mass of 40 to 60 M_{Jup}, or only 20 to 50 M_{Jup} according to D'Antona & Mazzitelli (1994; 1997). Also Woitas et al. (2001) give 20 to 40 M_{Jup} for GG Tau Bb using the D'Antona & Mazzitelli (1998) and Baraffe et al. (1998) models. We compared its properties with the Burrows et al. (1997) models, where the mass can be as low as ~ 23 M_{Jup}, so that we include the object in this study. Kinematic confirmation was done by White et al. (1999), who could determine the radial velocities of both GG Tau Ba and Bb to be 16.8 ± 0.7 km/s and 17.1 ± 1.0 km/s, i.e. consistent with each other and also with GG Tau A. The pair GG Tau A+B is also a common proper motion pair according to the NOMAD (Zacharias et al., 2005) and WDS catalogs (Mason et al., 2001). If accepted as planet, it would be the first planet imaged directly and confirmed by both common proper motion and spectroscopy. Orbital motion or curvature in orbital motion of GG Tau Bb around Ba were not yet reported.

TWA 5: The first direct imaging detection of the companion $1.960 \pm 0.006''$ (86.2 ± 4.0 AU) off TWA 5 (5 to 12 Myr as member of the TW Hya association, 44 ± 4 pc, M1.5) was done with NASA/IRTF and Keck/LRIS by Webb et al. (1999) and with HST/Nicmos and Keck/NIRC by Lowrance et al. (1999). The common proper motion and spectral (M8.5-9) confirmation was given in Neuhäuser, Guenther, Petr, Brandner, Huélamo & Alves (2000), who derived a mass of 15-40 M_{Jup} from formation models at the age and distance of the star. The mass lies anywhere between 4 and 145 M_{Jup}, if calculated from temperature (2800 ± 100 K), luminosity ($\log(L_{bol}/L_\odot) = -2.62 \pm 0.30$ at 44 ± 4 pc), and gravity ($\log g = 4.0 \pm 0.5$ cgs), as obtained by comparison of a VLT/Sinfoni K-band spectrum with Drift-Phoenix model atmospheres (Neuhäuser et al., 2009). The temperature error given in Neuhäuser et al. (2009) may be underestimated, because it is only from the K-band, so that we use a conservative, larger error here in Table 2. In our Table 2 below, we give 17 to 50 M_{Jup} as possible mass range. For any of those mass ranges, it might well be below 25 M_{Jup}, hence it is also a planet candidates imaged directly (called here TWA 5 B, but not b, in order not to confuse with TWA 5 Ab). Our latest image of TWA 5 A+B is shown in Fig. 1. Orbital motion of B around A was shown in Neuhäuser et al. (2010); the host star A is actually a very close 55 mas binary star. The data for separation and position angle plotted in Fig. 2 and 3 here are corrected for the binarity of the host star, i.e. are the values between the companion B and the photocenter of Aa+Ab using the orbit of Aa+b from Konopacky et al. (2007). What was plotted as orbital motion in figures 1 and 2 in Neuhäuser et al. (2010), actually is a small difference in proper motions of TWA

Object name	Luminosity $\log(L_{bol}/L_\odot)$	Magnitude M_K [mag]	Temp. T_{eff} [K]	Age [Myr]	Comments
Reference object (eSB2 brown dwarf - brown dwarf binary 2M0535):					
2M0535 A	-1.65 ± 0.07	5.29 ± 0.16	2715 ± 100	1 (0-3)	Stassun et al. (2007)
B	-1.83 ± 0.07	5.29 ± 0.16	2820 ± 105	1 (0-3)	Stassun et al. (2007)
Directly detected planet candidates:					
GG Tau Bb	-1.84 ± 0.32	6.28 ± 0.79	2880 ± 150	0.1-2	(1), (2)
TWA 5 B	-2.62 ± 0.30	8.18 ± 0.28	2800 ± 450	5-12	
GJ 417 B & C	-4.14 ± 0.06	11.74 ± 0.05	1600 ± 300	80-300	each object (1), (3)
GSC 08047 B/b	-3.58 ± 0.28	10.75 ± 0.60	2225 ± 325	25-40	
DH Tau B/b	-2.81 ± 0.32	8.46 ± 0.78	2750 ± 50	0.1-10	
GQ Lup b	-2.25 ± 0.24	7.37 ± 0.78	2650 ± 100	0.1-2	
2M1207 b	-4.74 ± 0.06	13.33 ± 0.12	1590 ± 280	5-12	
AB Pic B/b	-3.73 ± 0.09	10.82 ± 0.11	2000^{+100}_{-300}	25-40	(1)
LP 261-75 B/b	-3.87 ± 0.54	11.18 ± 1.34	1500 ± 150	100-200	(1)
HD 203030 B/b	-4.64 ± 0.07	13.14 ± 0.12	1440 ± 350	130-400	T_{eff} error (3)
HN Peg B/b	-4.93 ± 0.16	14.37 ± 0.25	1450 ± 300	200-300	(1), (3)
CT Cha b	-2.68 ± 0.21	8.86 ± 0.50	2600 ± 250	0.1-4	(7)
Fomalhaut b	≤ -6.5	$M_H \geq 23.5$		100-300	no colors/spectra
HR 8799 b	-5.1 ± 0.1	14.05 ± 0.08	1300 ± 400	20-1100	
c	-4.7 ± 0.1	13.13 ± 0.08	~ 1100	20-1100	
d	-4.7 ± 0.1	13.11 ± 0.12		20-1100	
e	-4.7 ± 0.2	12.93 ± 0.22		20-1100	
Wolf 940 B/b	-6.07 ± 0.04	18.36 ± 0.16	600 ± 100	3.5-6 Gyr	
G 196-3 B/b	$-3.8^{+0.2}_{-0.3}$	11.17 ± 0.62	1870 ± 100	20-600	
β Pic b	$-3.903^{+0.074}_{-0.402}$	11.20 ± 0.11	1700 ± 300	8-20	no spectra, (1), (4)
RXJ1609 B/b	-3.55 ± 0.20	10.36 ± 0.35	1800^{+200}_{-100}	5 (1-10)	
PZ Tel B/b	-2.58 ± 0.08	8.14 ± 0.15	2600 ± 100	8-20	(5), (1)
Ross 458 C	-5.62 ± 0.03	16.11 ± 0.05	650 ± 25	150-800	
GSC 06214 B/b	-3.09 ± 0.12	9.17 ± 0.23	2050 ± 450	5 (1-10)	(1), (3)
CD-35 2722 B/b	-3.59 ± 0.09	10.37 ± 0.16	1800 ± 100	50-150	(1)
HIP 78530 B/b	-2.55 ± 0.13	8.19 ± 0.18	2800 ± 200	5 (1-10)	
WD 0806-661 B/b		$M_J \geq 21.7$	300	1.5-2.7 Gyr	(6)
SR 12 C	-2.87 ± 0.20	9.09 ± 0.44	2400^{+155}_{-100}	0.3-10	
HR 7329 B/b	-2.63 ± 0.09	8.21 ± 0.12	2650 ± 150	8-20	

Table 1. Observed properties of the directly imaged planet candidates. References given in Sect. 5 (1) luminosity from spectral type (BC from Golimowski et al. (2004)), K magnitude and distance (2) temperature from spectral type using Luhman et al. (2003) (3) temperature from spectral type using Golimowski et al. (2004) (4) temperature from Ks - L' color (5) temperature from JHK colors (6) detected at 4.5 μm (7) Only for CT Cha b extinction was taken into account as given in Schmidt et al. (2008)

5 A and B, so small, that it is consistent with the expected orbital motion; figures 1 and 2 in Neuhäuser et al. (2010) only show a linear fit. However, true orbital motion cannot be linear, but always shows some curvature. In figure 3 in Neuhäuser et al. (2010), it is shown from geometric fits that an eccentric orbit of B around A is most likely, hence curvature is detected (with low significance). Curvature is not yet a final proof for being bound, because it would also be expected for an hyperblic orbit. The orbital period is $\sim$ 950 yr (for a circular orbit) or $\sim$ 1200 yr for an eccentric orbit with the best fit eccentricity $e = 0.45$ (Neuhäuser et al., 2010).

GJ 417: Common proper motion between the binary star GJ 417 (or Gl 417, CCDM J11126+3549AB, WDS J11125+3549AB, called primary A in Bouy et al. (2003)) and the companion 2MASS J1112256+354813 was noticed by Bouy et al. (2003). The primary, GJ 417, is comprised by two stars both with spectral type G0 (Simbad). This primary GJ 417 A (or GJ 417 Aa+b) has common proper motion with 2MASS J1112256+354813 at a wide separation of $\sim$ 90$''$ (or $\sim$ 1953 AU at $\sim$ 21.7 pc, Bouy et al. (2003)). The secondary, 2MASS J1112256+354813, is a close binary itself (called B and C in Bouy et al. (2003)) with $\sim$ 0.0700$''$ separation with almost equal magnitudes and a combined spectral type of L4.5 (Bouy et al., 2003). At the distance of GJ 417, this separation corresponds to only $\sim$ 1.5 AU projected separation and a very short period of few years. The age of the system is given to be only 80 to 300 Myr (Faherty et al., 2010), so that the mass of B and C can be near the planetary mass regime (Faherty et al., 2010).

GSC 08047 (GSC 08047-00232): The first direct imaging detections of this companion 3.238 $\pm$ 0.022$''$ (219 $\pm$ 59 AU) off GSC 08047 (K2, 50-85 pc, 25 to 40 Myr as member of the TucHor Association) was shown in Neuhäuser et al. (2003) using simple IR imaging with NTT/SofI and IR speckle imaging with NTT/Sharp as well as in Chauvin et al. (2003) with AO imaging using NTT/Adonis. Neuhäuser & Guenther (2004) could show common proper motion, while both Neuhäuser & Guenther (2004) and Chauvin, Lagrange, Lacombe, Dumas, Mouillet, Zuckerman, Gendron, Song, Beuzit, Lowrance & Fusco (2005) presented spectra (M6-9.5). Based on formation models, Neuhäuser & Guenther (2004) derived the mass of the companion to be 7-50 M_{Jup} at the age and distance of the star.

DH Tau: Direct imaging AO detection with Subaru/CIAO of the companion 2.351 $\pm$ 0.001$''$ ($\sim$ 329 AU) off DH Tau (0.1 to 10 Myr and at $\sim$ 140 pc as member of the Taurus T association, M0.5) were given in Itoh et al. (2005), who also could show common proper motion and a high-resolution spectrum with Subaru/CISCO giving temperature and gravity yielding a mass of 30-50 M_{Jup}. A small difference observed in the position angle is consistent with orbital motion (Itoh et al., 2005).

GQ Lup: Direct imaging AO detection with VLT/NACO of the companion 0.7347 $\pm$ 0.0031$''$ ($\sim$ 100 AU) off GQ Lup (0.1 to 2 Myr and at $\sim$ 140 pc as member of the Lupus-I T association, K7) together with common proper motion, spectral classification (late-M to early-L), and a mass estimate of 1-42 M_{Jup} (Neuhäuser et al., 2005) were confirmed by Janson et al. (2006) giving a mass of 3-20 M_{Jup}, Marois et al. (2007) deriving 10-20 M_{Jup}, and McElwain et al. (2007) listing 10-40 M_{Jup}, all from photometry and temperature of the companion, age, and distance of the star, together with formation models. Seifahrt et al. (2007) obtained higher-resolution VLT/Sinfoni spectra to derive the gravity of the companion and determined the mass model-independant to be 4-155 M_{Jup}. Evidence for a few mas/yr orbital motion (Neuhäuser et al., 2008) does not yet show curvature. Hence, the companion to GQ Lup can be a massive planet or a low-mass brown dwarf.

2M1207 (2MASSWJ1207334-393254): While the first direct imaging AO detection with VLT/NACO of this companion $0.7737 \pm 0.0022''$ (40.5 ± 1 AU) off the brown dwarf 2M1207 A (5 to 12 Myr as member of the TW Hya Association, 52.4 ± 1.1 pc, M8 brown dwarf) was published in Chauvin et al. (2004), the proper motion confirmation was given in Chauvin, Lagrange, Dumas, Zuckerman, Mouillet, Song, Beuzit & Lowrance (2005). Mugrauer et al. (2005) and Close et al. (2007) noticed that the binding energy between 2M1207 and its companion may not be sufficient for being bound or for staying bound for a long time: The total mass is too low for the large separation. Orbital motion or curvature in the orbital motion were not yet shown. The companion also appears to be too faint given its L5-L9.5 spectral type and 5 to 12 Myr age (Mohanty et al., 2007).

AB Pic: The first direct imaging AO detection with VLT/NACO of this companion $5.460 \pm 0.014''$ (251.7 ± 8.9 AU) off AB Pic (46.1 ± 1.5 pc, K1, 25 to 40 Myr as member of the TucHor Association) together with spectrum (L0-2), proper motion confirmation, and a mass estimate based on formation models to be 13-14 M_{Jup} were published in Chauvin, Lagrange, Zuckerman, Dumas, Mouillet, Song, Beuzit, Lowrance & Bessell (2005). Bonnefoy et al. (2010) obtained temperature and gravity with VLT/Sinfoni spectra and estimated the mass to be 1 to 45 M_{Jup}.

LP 261-75: Reid & Walkowicz (2006) noticed this common proper motion pair: The companion 2MASSW J09510549+3558021 (or LP 261-75 B) has a separation of $\sim 12''$ (~ 744 AU) off LP 261-75 (62 ± 38 pc, M4.5, 100 to 200 Myr due to its activity). Reid & Walkowicz (2006) presented a spectrum of the companion (L6), showed proper motion confirmation, and estimated the mass based on formation models to be 15-30 M_{Jup}.

HD 203030: The first direct imaging AO detection with Palomar of this companion $11.923 \pm 0.021''$ (503 ± 15 AU) off HD 203030 (42.2 ± 1.2 pc, G8, 130 to 400 Myr due to its activity) together with spectrum (L7-8), proper motion confirmation, and a mass estimate based on formation models to be 12-31 M_{Jup} were published in Metchev & Hillenbrand (2006).

HN Peg: First direct imaging detection with 2MASS and Spitzer/IRAC of this companion $43.2 \pm 0.4''$ (773 ± 13 AU) off HN Peg (17.89 ± 0.14 pc, G0, 200 to 300 Myr, if a member of the Her-Lyr group) together with common proper motion confirmation were shown in Luhman et al. (2007). Given the NASA/IRTF/SpecX spectral detection of methane, the companion can be classified T2.5 $\pm$ 0.5, so that it has 12-30 M_{Jup} at the age and distance of the star. The large projected separation of ~ 773 AU may favor the brown dwarf interpretation.

CT Cha: First direct imaging AO detection with VLT/NACO of this companion $2.670 \pm 0.036''$ (441 ± 87 AU) off CT Cha (165 ± 30 pc and 0.1 to 4 Myr as member of the Cha I T association, K7) together with VLT/Sinfoni JHK spectra (M8-L0), common proper motion confirmation, and a mass estimate based on formation models to be 11-23 M_{Jup} at the age and distance of the star were published in Schmidt et al. (2008), so that this companion can also be a high-mass planet or low-mass brown dwarf.

Fomalhaut b: Direct imaging detection in the red optical with the Hubble Space Telescope (HST) of this companion $12.7''$ (~ 100 AU) off Fomalhaut (7.704 ± 0.028 pc, A4, 100 to 300 Myr old) together with common proper motion confirmation were published in Kalas et al. (2008). They also estimated the mass of the companion to be below ~ 3 M_{Jup} due to its location close to the dusty debris disk seen in reflected optical light. Kalas et al. (2008) also obtained a few imaging photometric points and upper limits; those data points were not consistent with the

expected spectrum of a low-mass cool planet, so that they could not exclude that the emission is reflected light from the small cloud-let. A spectrum or an IR detection of the companion could not yet be obtained. After two imaging epochs, the slightly different positions of the companion with respect to the star are consistent with orbital motion (Kalas et al., 2008), but curvature in the orbital motion was not yet shown.

HR 8799: Direct imaging AO detection with Keck/NIRC2 and Gemini North/NIRI of the companions b, c, and d was shown by Marois et al. (2008) together with common proper motion confirmation for all three companions, while orbital motion could be shown for companions b and c. The orbital motion confirmation of the third candidate, d, was later given with higher significance by Metchev et al. (2009). A fourth candidate, HR 8799 e, was later detected by Marois et al. (2010), whose orbital (and common proper motion, however no significance is explicitly given for this) with the star was shown within this publication. The companions b, c, d, and e have separations of $1.713 \pm 0.006''$, $0.952 \pm 0.011''$, $0.613 \pm 0.026''$, and $0.362 \pm 0.033''$, respectively, which correspond to 14 to 67 AU at the distance of the star being 39.4 ± 1.0 pc, similar as the solar system dimension. Spectra were taken for HR 8799 b by Bowler et al. (2010) and Barman et al. (2011) and for HR 8799 c by Janson et al. (2010), showing tempartures of $1300 - 1700$ K and 1100 ± 100 K for HR 8799 b and ~ 1100 K for HR 8799 c, respectively. The age of the star is somewhat uncertain: Given its bright debris disk, it might be as young as 20 Myr, then the companions are certainly below 13 M_{Jup}; astroseismology, however, seem to indicate that the star can be as old as ~ 1.1 Gyr, then the companions would be brown dwarfs.

Wolf 940: The first imaging detection in UKIDSS, later also detected with Keck AO and laser guide star, of this companion $32''$ (~ 400 AU) off Wolf 490 (12.53 ± 0.71 pc, 3.5-6 Gyr due to activity, M4) was presented by Burningham et al. (2009) together with common proper motion and spectra (T8.5). Comparison of their spectra with BT Settl models yields 500 to 700 K, while the temperature and gravity estimates also given in Burningham et al. (2009), 570 ± 25 K, are obtained using the radius from cooling models for the age range from the stellar activity, hence possibly less reliable. A mass was also obtained from models for the given age range, namely 20-32 M_{Jup} (Burningham et al., 2009).

G 196-3: The first direct imaging detection of the companion $\sim 16.2''$ (243-437 AU) off G186-3 (host star: M2.5V, 20 to 600 Myr, 15-27 pc) was published by Rebolo et al. (1998) using the 1m NOT/ALFOSC and HiRAC instruments in the red optical and IR without AO, together with common proper motion ($2\,\sigma$ only) and spectroscopic (L3) confirmation. The mass was estimated to be 15-40 M_{Jup} or 12-25 M_{Jup} from cooling models for 20 to 600 Myr (Rebolo et al., 1998) or 20 to 300 Myr (Zapatero Osorio et al., 2010). if the $2\,\sigma$ common proper motion is accepted as confirmation, then is would actually be the first imaged planet (candidate) confirmed as co-moving companion by proper motion (Rebolo et al., 1998); higher significance for common proper motion was presented by Zapatero Osorio et al. (2010).

β Pic: The first direct imaging AO detection with VLT/NACO of this companion $0.441 \pm 0.008''$ (8.57 ± 0.18 AU) off β Pic (19.440 ± 0.045 pc, 8 to 20 Myr, A6) was presented in Lagrange et al. (2009), while the 2nd epoch image with common proper motion confirmation was presented in Lagrange et al. (2010). This planet detected at ~ 10 AU projected separation was predicted before by Freistetter et al. (2007) at ~ 12 AU semi-major axis with ~ 2-5 M_{Jup} to account for the main warp, the two inner belts, and the falling evaporaing bodies in the β Pic debris disk. Lagrange et al. (2009) estimated the mass of the detected object to be ~ 6-13 M_{Jup}

based on uncertain formation models at the age and distance of the star. A spectrum of the companion could not yet be obtained. After two imaging epochs, the different positions of the companion with respect to the star are consistent with orbital motion (Lagrange et al., 2010), but the object can still be a moving background object.

RXJ 1609 (1RXS J160929.1-210524): The first direct imaging AO detection with Gemini of this companion $2.219 \pm 0.006''$ (~ 311 AU) off RXJ1609 (~ 145 pc and 1 to 10 Myr as member of the Sco-Cen T association, K7-M0) was presented by Lafrenière et al. (2008), while the common proper motion confirmation was published by Lafrenière et al. (2010) and also confirmed by Ireland et al. (2011). From the JHK Gemini/NIRI spectra (with the AO system Altair), Lafrenière et al. (2008; 2010) obtained a spectral type (L2-5) and temperature, and with age and distance of the star, a mass estimate of 6-11 M_{Jup} from uncertain formation models.

PZ Tel: The first direct imaging AO detections of this companion $0.3563 \pm 0.0011''$ (18.35 ± 0.99 AU) off the star PZ Tel (51.5 ± 2.6 pc, 8 to 20 Myr as member of the β Pic moving group, G9) were obtained with Gemini/NICI by Biller et al. (2010) and with VLT/NACO by Mugrauer et al. (2010). They both could also confirm common proper motion. They estimate the mass of PZ Tel B to be 30-42 or 24-40 M_{Jup}, respectively, again possibly below 25 M_{Jup}, so that this companion could be classified as planetary companion imaged directly. Mugrauer et al. (2010) not only show common proper motion between A and B with $\geq 39\,\sigma$, but also orbital motion of B around A with $\geq 37\,\sigma$ including curvature of orbital motion at $2\,\sigma$ significance.

Ross 458 C: The imaging detection of the companion C (possibly also to be called b as planet candidate) to the host star binary Ross 458 A+B (12 pc, M0+M7 pair, 150 to 800 Myr) was published in Goldman et al. (2010) and Scholz (2010) using the 3.5m UKIRT Infrared Deep Sky Survey together with common proper motion confirmation, with the separation of Ross C being $102''$ or 1100 AU. The spectroscopic (T8) confirmation was presented in Burgasser et al. (2010) using the 6.5m Magellan/FIRE. The mass of C is estimated to be $\sim 14\,M_{Jup}$ from magnitude, temperature, and gravity of the companion at the distance of the host star (Burgasser et al., 2010).

GSC 06214 (GSC 06214-00210): The first direct imaging detections with the 200-inch Palomar/PHARO and the 10-m Keck/NIRC2 detectors, using a combination of conventional AO imaging and non-redundant mask interferometry (sparse aperture mask with AO) of this companion $2.2033 \pm 0.0015''$ (i.e. 319 ± 31 AU) off the star GSC 06214 (1 to 10 Myr and 145 ± 14 pc as member of ScoCen T association, M1) together with common proper motion confirmation was published by Ireland et al. (2011), who estimate the mass of the companion from its colors (neglecting extinction, M8-L4), the distance and age of the star, and cooling models to be $\sim 10\text{-}15\,M_{Jup}$.

CD-35 2722: The first direct imaging AO detections with Gemini-S/NICI of this companion $3.172 \pm 0.005''$ (i.e. 67.56 ± 4.6 AU) off the star CD-35 2722 (50 to 150 Myr as member of the AB Dor moving group, 21.3 ± 1.4 pc, M1) together with common proper motion confirmation and spectral classification as $L4 \pm 1$ were published by Wahhaj et al. (2011), who estimate the mass of the companion from its luminosity, the age of the star, and cooling models to be $31 \pm 8\,M_{Jup}$, or lower when using the temperature of the companion, so that it could be a planet imaged directly. As shown by Wahhaj et al. (2011), the fact that the position angle of this companion compared to the host star does not change signficantly is inconsistent with a non-moving background object by $3\,\sigma$; the fact that at the same time the separation between

companion and host star does change signficantly, namely exactly according to what would be expected for a non-moving background object, can either be interpreted as concern (really co-moving ?) or as evidence for orbital motion: No change in position angle, but small change in separation would indicate that the orbit is either seen edge-on and/or strongly eccentric; it is of course also possible that the faint object is a moving background object or another, but independent, young member of the AB Dor group.

HIP 78530: The first direct imaging AO detection with Gemini/NIRI of this companion $4.529 \pm 0.006''$ (i.e. 710 ± 60 AU) off HIP 78530 (1 to 10 Myr as member of the ScoCen OB association, B9, 157 ± 13 pc) together with common proper motion confirmation and spectroscopy (M8 $\pm$ 1) were published by Lafrenière et al. (2011), who determined the mass from formation models to be 19-26 M_{Jup}. HIP 78530 is so far the most massive host star with directly imaged planet (candidate).

WD 0806-661: The first direct (normal IR) imaging detections with the Spitzer Infrared Array Camera at 4.5 μm of this companion $103.2 \pm 0.2''$ (i.e. ~ 2500 AU) off the White Dwarf WD 0806-661 (~ 1.5 Gyr, 19.2 ± 0.6 pc) together with common proper motion confirmation was published by Luhman et al. (2011). From the companion brightness at 4.5 μm and the rough age of the host star (WD age plus progenitor life time), Luhman et al. (2011) estimate the mass of the companion to be ~ 7 M_{Jup}. Rodriguez et al. (2011) argue that the host star age (WD plus progenitor) can be as large as ~ 2.7 Gyr, so that the companion mass can be as large as ~ 13 M_{Jup}, still in the planetary mass range.

SR 12: Direct imaging detection with Subaru/CIAO of the companion SR 12 C (possibly to be called SR 12 b as planetary companion) $8.661 \pm 0.033''$ (1300 ± 220 AU) off the close binary SR 12 A+B (K4+M2.5, 125 ± 25 pc and 0.3-10 Myr as member of the ρ Oph star forming cloud) together with significant common proper motion confirmation (their figure 4 with five epochs) and a spectrum (M8.5-9.5) were published in Kuzuhara et al. (2011); they derived a mass of SR 12 C to be 6-20 M_{Jup}. Given the large separation inside the ρ Oph cloud, the object C could also be an independant member of the cloud. Orbital motion or curvature in orbital motion were not yet detected.

HR 7329: Direct imaging detection with HST/Nicmos of the companion (one epoch) $4.194 \pm 0.016''$ (200 ± 16 AU) off HR 7329 (η Tel, A0, 47.7 ± 1.5 pc, 8 to 20 Myr as member of the β Pic moving group) and a spectrum (M7-8) were published in Lowrance et al. (2000). Common proper motion between HR 7329 A and B/b was shown convincingly (above 3 σ) only recently with new AO imaging (Neuhäuser et al., 2011).

We notice that the objects GG Tau Bb, TWA 5 B, GJ 417 B & C, GSC 08047 B/b, LP 261-75 B/b, HD 203030 B/b, Wolf 940 B/b, G196-3 B/b, PZ Tel B/b, HR 7329 B/b, were not yet listed in Schneider et al. (2011) nor www.exoplanet.eu. We also note that the object CHXR 73 b (Luhman et al., 2006) listed in Schneider et al. (2011) and www.exoplanet.eu as planet imaged directly, is not included in our listing, because common proper motion has not been shown, yet. A few sub-stellar, possibly planetary mass companions to brown dwarfs, listed as possible planets in Schneider et al. (2011) and www.exoplanet.eu, are also not listed in this paper, because they are probably not bound, namely Oph J1622-2405 (also called Oph 1622 or Oph 11, Jayawardhana & Ivanov (2006), UScoCTIO-108 (Béjar et al., 2008), 2MASS J04414489+2301513 (Todorov et al., 2010), and CFBDIRJ1458+1013 AB (also called CFBDS 1458,
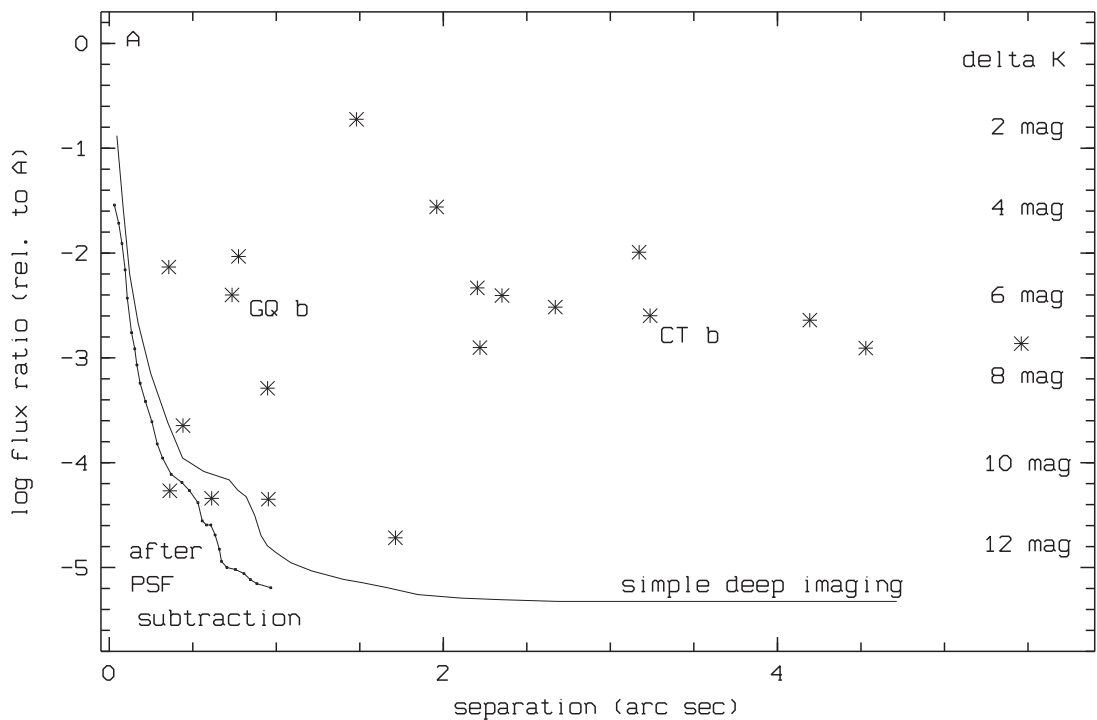
Fig. 4. We plot the (log of the) flux ratio between the noise level (S/N=3) and the primary host star (left y axis) or the K-band magnitude difference (right y axis) versus the separation between companion and host star (in arc sec). The primary host star is indicated in the upper left by the letter A (log of flux ratio and separation being zero). The flux ratios of all 20 companions listed in Tables 1 and 2 with separations up to 6″ and known K-band flux ratio (known for all but Fomalhaut) are plotted as star symbols (references for K-band magnitudes for the stars and their companions and for the separations between them can be found in Sect. 5). The companions discovered by us (GQ Lup b and CT Cha b) are indicated. The curve is the dynamic range achieved in our deep AO imaging on GQ Lup with 102 min total integration time with VLT/NACO; the lower curve with dots is the dynamic range for the same data achieved after PSF subtraction (figure adapted from figure 7 in Neuhäuser et al. (2008)). All companions above the curve(s) can be detected by this (simple AO imaging) method. Companions that are fainter and/or closer, i.e. below the curve, cannot be detected. The PSF subtraction technique can improve the dynamic range and detection capability at 0.5 to 1″ by about one magnitude. The only two companions below the upper dynamic range curve (before PSF subtraction) are HR 8799 d and e, which were detected by the ADI technique (Marois et al., 2008; 2010). Error bars are omitted for clarity.

Liu et al. (2011)). 2M1207 should therefore also not be listed here; however, we do include it for completness and comparison, because it is often included in lists of planets imaged directly.
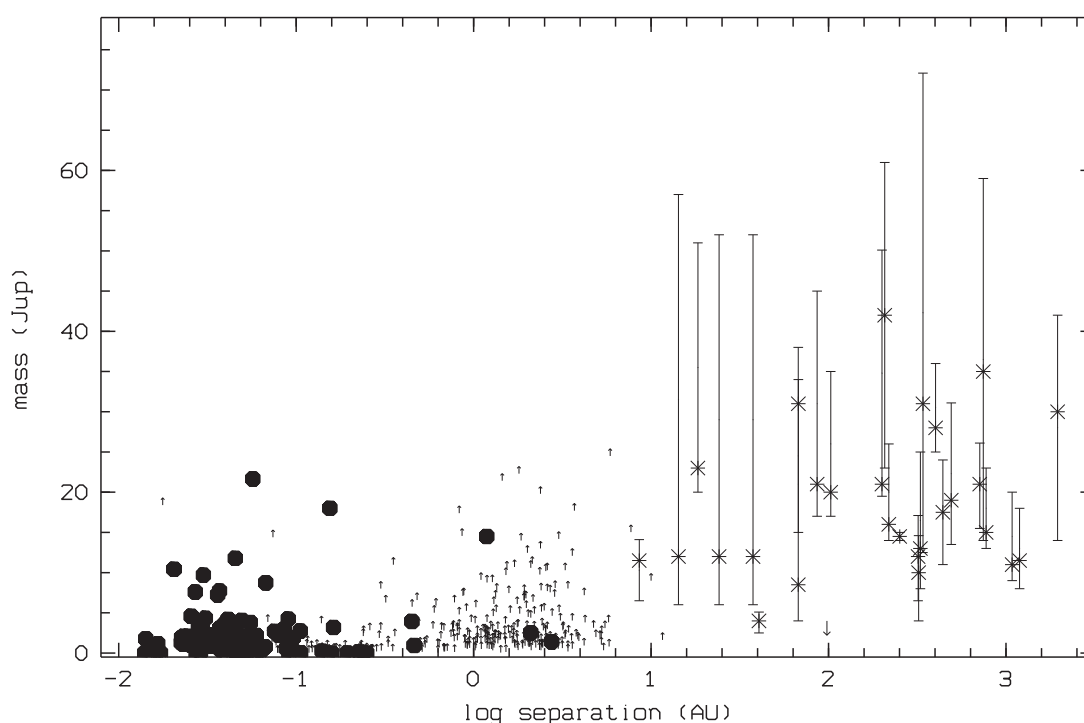
Fig. 5. We plot the mass of the companion (in Jupiter masses) versus the (log of the) separation (in AU) for (i) planet candidates detected by radial velocity only (lower mass limits plotted), (ii) radial velocity planets confirmed by either astrometry or transit (filled symbols), where the true masses are known, and (iii) planets and candidates detected by direct imaging (star symbols) with masses from the Burrows et al. (1997) model as in Tables 2, because only the Burrows et al. model gives a correct mass for the eSB2 brown dwarf 2M0535 B, and projected physical separations (calculated from angular separations and distances as given in Sect. 5); for Fomalhaut b, we plot few M_{Jup} as upper mass limit at ~ 100 AU; only WD 0806-661 is not plotted, because we could not determine its mass in the same (homogeneous) way as for the others, since the WD 0806-661 companion is detected only at 4.5 μm, but not in the near-IR. The four radial velocity planets with the largest separations (8.9 to 11.6 AU) are ν Oph c, HIP 5158 c, HIP 70849 b and 47 UMa d. The directly detected planets (or candidates) with the smallest projected separations (8.6 to 18.3 AU) are β Pic b, HR 8799 e, and PZ Tel b; these systems are all younger than ~ 100 Myr, so that the companions are still bright enough for direct detection. This plot shows that the parameter regimes, in which the radial velocity technique and the direct imaging technique are working, are about to overlap. This is due to longer monitoring periods for the radial velocity technique and due to improved technology and, hence, dynamic range in direct imaging. Hence, it might soon be possible to observe the same planets with both direct imaging and radial velocity, which would be best possible for young nearby systems. The data for radial velocity, transit, and astrometry planets were taken from www.exoplanet.eu (on 28 July 2011), where the references for those planets can also be found. We omitted most error bars for clarity, but we do show the mass errors for the directly imaged planets and candidates.

Object name	Burrows 97 (L, age)	Chabrier 00 (L, M_K, T, t)	Baraffe 03 (L, M_K, T, t)	Marley 07 ($\leq$ 10 Jup)	Baraffe 08 ($\geq$ 10 Myrs)	Wuchterl (Neuh05)
Reference object (eSB2 brown dwarf - brown dwarf binary 2M0335):					
2M0535 A	50 (45-60)	55 (30-60)	50 (45-80)			5-13
B	37 (33-46)	45 (40-50)	43 (40-65)			$\leq$ 13
Directly detected planet candidates:					
GG Tau Bb	42 (23-61)	52 ($\geq$ 35)	56 ($\geq$ 41)			
TWA 5 B	21 (17-45)	23 (20-50)	25 (20-50)			
GJ 417 B & C	30 (14-42)	26 (18-35)	25 (20-35)			
GSC 08047 B/b	16 (14-26)	19 (17-25)	18 (14-25)			
DH Tau B/b	13 (8-25)	20 (6-47)	20 (6-50)	10 ($\geq$ 7)		5
GQ Lup b	20 (17-35)	25 (20-35)	27 (24-37)			1-5
2M1207 b	4 (2.5-5)	5 (2.5-13)	5 (2.5-12)	4 (3-5)	4	
AB Pic B/b	14.5 (14-15)	16 (14-18)	15.5 (11-17)			
LP 261-75 B/b	35 (14-59)	26 (16-30)	28 (16-32)			
HD 203030 B/b	19 (13.5-31)	24 (13-28)	23 (11-26)			
HN Peg B/b	15 (13-23)	21 (14-31)	20 (13-27)	$\geq$ 10		
CT Cha b	17.5 (11-24)	14 (13-19)	16 (13-21)			2-5
Fomalhaut b	$\leq$ 4.25		$\leq$ 2	$\leq$ 3	$\leq$ 2	
HR 8799 b	8.5 (4-38)	13 (3-63)	12 (4-32)	7 ($\geq$ 3)	7 ($\geq$ 3)	
c	12 (6-52)	16 (5-42)	12 (6-42)	10 ($\geq$ 6)	$\geq$ 5	
d	12 (6-52)	16 (5-42)	12 (6-42)	10 ($\geq$ 6)	$\geq$ 5	
e	12 (6-57)	16 (5-42)	12 (6-42)	10 ($\geq$ 6)	$\geq$ 5	
Wolf 940 B/b	28 (25-36)		33 (24-43)			
G 196-3 B/b	31 (12.5-72)	44 (14-60)	43 (11-55)			
β Pic b	11.5 (6.5-14)	10 (6-17)	9.5 (8-11)	10 ($\geq$ 9)	9 ($\geq$ 8)	
RXJ1609 B/b	10 (4-14.5)	8 (4-14)	8 (4-13)	8 ($\geq$ 4)		
PZ Tel B/b	23 (20-51)	28 (21-41)	28 (24-41)			
Ross 458 C	11.5 (8-18)		13 (8-15)			
GSC 06214 B/b	12 (6.5-17)	15 (6-18)	14 (6-23)			
CD-35 2722 B/b	31 (15-34)	35 (16-43)	31 (16-41)			
HIP 78530 B/b	21 (15.5-26)	30 (13-84)	32 (11-93)			
WD 0806-661 B/b			$\leq$ 8.5			
SR 12 C	11 (9-20)	10 (5-25)	10 (6-25)	10 ($\geq$ 8)		2-5
HR 7329 B/b	21 (19.5-50)	26 (21-43)	27 (23-36)			

Table 2. Masses derived from evolutionary hot-start models.

6. Conclusion

We noticed that the Burrows et al. (1997) models give correct masses for 2M0535 B, a young brown dwarf in the eclipsing double-lined spectroscopic brown dwarf - brown dwarf binary system in Orion, where masses have been determined without model assumptions (Stassun et al., 2006; 2007). Hence, we apply this model for best mass estimates for the planets and candidates imaged directly, see Fig. 5.

We conclude that direct imaging detection of planets around other stars is possible since several years with both ground-based AO IR imaging and space-based optical imaging. For most planets and candidates imaged and confirmed as companions by common proper motion so far, the planet status is still dubious. Possibly planetary mass companions apparently co-moving with brown dwarfs, i.e. apparently forming very wide very low-mass binaries, may well be unbound, i.e. currently flying apart (Mugrauer et al. (2005),Close et al. (2007)).

Extra-solar planets or candidates as close to their host star as the Solar System planets (within 30 AU) are still very rare with β Pic b, HR 8799 e, PZ Tel B/b, and HR 8799 d being the only exceptions at 8.5, 14.3, 18.3, and 24.2 AU, respectively, all nearby young stars (19 to 52 pc). As far as angular separation is concerned, the closest planets or candidates imaged directly are PZ Tel B/b, HR 8799 e, β Pic b, HR 8799 d, and GQ Lup b with separations from 0.36 to 0.75 arc sec.

New AO imaging techniques like ADI, SAM, and locally optimized combination of images have improved the ability to detect such planets. Future AO instruments at 8-meter ground-based telescopes will improve the accessible dynamic range even further. Imaging with a new space based telescope like JWST (Beichman et al., 2010) or AO imaging at an extremely large telescope of 30 to 40 meters would improve the situation significantly. Imaging detection of planets with much lower masses, like e.g. Earth-mass planets, might be possible with a space-based interferometer like Darwin or TPF, but also only around very nearby stars.

7. References

Absil, O. & Mawet, D. (2010). Formation and evolution of planetary systems: the impact of high-angular resolution optical techniques, *A&AR* 18: 317–382.

Baraffe, I., Chabrier, G., Allard, F. & Hauschildt, P. H. (1998). Evolutionary models for solar metallicity low-mass stars: mass-magnitude relationships and color-magnitude diagrams, *A&A* 337: 403–412.

Barman, T. S., Macintosh, B., Konopacky, Q. M. & Marois, C. (2011). Clouds and Chemistry in the Atmosphere of Extrasolar Planet HR8799b, *ApJ* 733: 65–+.

Beichman, C. A., Krist, J., Trauger, J. T., Greene, T., Oppenheimer, B., Sivaramakrishnan, A., Doyon, R., Boccaletti, A., Barman, T. S. & Rieke, M. (2010). Imaging Young Giant Planets From Ground and Space, *PASP* 122: 162–200.

Béjar, V. J. S., Zapatero Osorio, M. R., Pérez-Garrido, A., Álvarez, C., Martín, E. L., Rebolo, R., Villó-Pérez, I. & Díaz-Sánchez, A. (2008). Discovery of a Wide Companion near the Deuterium-burning Mass Limit in the Upper Scorpius Association, *ApJL* 673: L185–L189.

Benedict, G. F., McArthur, B. E., Forveille, T., Delfosse, X., Nelan, E., Butler, R. P., Spiesman, W., Marcy, G., Goldman, B., Perrier, C., Jefferys, W. H. & Mayor, M. (2002). A Mass for the Extrasolar Planet Gliese 876b Determined from Hubble Space Telescope Fine Guidance Sensor 3 Astrometry and High-Precision Radial Velocities, *ApJL* 581: L115–L118.

Benedict, G. F., McArthur, B. E., Gatewood, G., Nelan, E., Cochran, W. D., Hatzes, A., Endl, M., Wittenmyer, R., Baliunas, S. L., Walker, G. A. H., Yang, S., Kürster, M., Els, S. & Paulson, D. B. (2006). The Extrasolar Planet ϵ Eridani b: Orbit and Mass, *AJ* 132: 2206–2218.

Biller, B. A., Liu, M. C., Wahhaj, Z., Nielsen, E. L., Close, L. M., Dupuy, T. J., Hayward, T. L., Burrows, A., Chun, M., Ftaclas, C., Clarke, F., Hartung, M., Males, J., Reid, I. N., Shkolnik, E. L., Skemer, A., Tecza, M., Thatte, N., Alencar, S. H. P., Artymowicz, P., Boss, A., de Gouveia Dal Pino, E., Gregorio-Hetem, J., Ida, S., Kuchner, M. J., Lin, D. & Toomey, D. (2010). The Gemini NICI Planet-finding Campaign: Discovery of a Close Substellar Companion to the Young Debris Disk Star PZ Tel, *ApJL* 720: L82–L87.

Bonnefoy, M., Chauvin, G., Rojo, P., Allard, F., Lagrange, A.-M., Homeier, D., Dumas, C. & Beuzit, J.-L. (2010). Near-infrared integral-field spectra of the planet/brown dwarf companion AB Pictoris b, *A&A* 512: A52+.

Bouy, H., Brandner, W., Martín, E. L., Delfosse, X., Allard, F. & Basri, G. (2003). Multiplicity of Nearby Free-Floating Ultracool Dwarfs: A Hubble Space Telescope WFPC2 Search for Companions, *AJ* 126: 1526–1554.

Bowler, B. P., Liu, M. C., Dupuy, T. J. & Cushing, M. C. (2010). Near-infrared Spectroscopy of the Extrasolar Planet HR 8799 b, *ApJ* 723: 850–868.

Burgasser, A. J., Simcoe, R. A., Bochanski, J. J., Saumon, D., Mamajek, E. E., Cushing, M. C., Marley, M. S., McMurtry, C., Pipher, J. L. & Forrest, W. J. (2010). Clouds in the Coldest Brown Dwarfs: Fire Spectroscopy of Ross 458C, *ApJ* 725: 1405–1420.

Burningham, B., Pinfield, D. J., Leggett, S. K., Tinney, C. G., Liu, M. C., Homeier, D., West, A. A., Day-Jones, A., Huelamo, N., Dupuy, T. J., Zhang, Z., Murray, D. N., Lodieu, N., Barrado Y Navascués, D., Folkes, S., Galvez-Ortiz, M. C., Jones, H. R. A., Lucas, P. W., Calderon, M. M. & Tamura, M. (2009). The discovery of an M4+T8.5 binary system, *MNRAS* 395: 1237–1248.

Burrows, A., Marley, M., Hubbard, W. B., Lunine, J. I., Guillot, T., Saumon, D., Freedman, R., Sudarsky, D. & Sharp, C. (1997). A Nongray Theory of Extrasolar Giant Planets and Brown Dwarfs, *ApJ* 491: 856–+.

Charbonneau, D., Brown, T. M., Latham, D. W. & Mayor, M. (2000). Detection of Planetary Transits Across a Sun-like Star, *ApJL* 529: L45–L48.

Chauvin, G., Lagrange, A.-M., Dumas, C., Zuckerman, B., Mouillet, D., Song, I., Beuzit, J.-L. & Lowrance, P. (2004). A giant planet candidate near a young brown dwarf. Direct VLT/NACO observations using IR wavefront sensing, *A&A* 425: L29–L32.

Chauvin, G., Lagrange, A.-M., Dumas, C., Zuckerman, B., Mouillet, D., Song, I., Beuzit, J.-L. & Lowrance, P. (2005). Giant planet companion to 2MASSW J1207334-393254, *A&A* 438: L25–L28.

Chauvin, G., Lagrange, A.-M., Lacombe, F., Dumas, C., Mouillet, D., Zuckerman, B., Gendron, E., Song, I., Beuzit, J.-L., Lowrance, P. & Fusco, T. (2005). Astrometric and spectroscopic confirmation of a brown dwarf companion to GSC 08047-00232. VLT/NACO deep imaging and spectroscopic observations, *A&A* 430: 1027–1033.

Chauvin, G., Lagrange, A.-M., Zuckerman, B., Dumas, C., Mouillet, D., Song, I., Beuzit, J.-L., Lowrance, P. & Bessell, M. S. (2005). A companion to AB Pic at the planet/brown dwarf boundary, *A&A* 438: L29–L32.

Chauvin, G., Thomson, M., Dumas, C., Beuzit, J.-L., Lowrance, P., Fusco, T., Lagrange, A.-M., Zuckerman, B. & Mouillet, D. (2003). Adaptive optics imaging survey of the Tucana-Horologium association, *A&A* 404: 157–162.

Close, L. M., Zuckerman, B., Song, I., Barman, T., Marois, C., Rice, E. L., Siegler, N., Macintosh, B., Becklin, E. E., Campbell, R., Lyke, J. E., Conrad, A. & Le Mignant, D. (2007). The Wide Brown Dwarf Binary Oph 1622-2405 and Discovery of a Wide, Low-Mass Binary in Ophiuchus (Oph 1623-2402): A New Class of Young Evaporating Wide Binaries?, *ApJ* 660: 1492–1506.

D'Antona, F. & Mazzitelli, I. (1994). New pre-main-sequence tracks for M less than or equal to 2.5 solar mass as tests of opacities and convection model, *ApJS* 90: 467–500.

D'Antona, F. & Mazzitelli, I. (1997). Evolution of low mass stars, *MdSAI* 68: 807–+.

D'Antona, F. & Mazzitelli, I. (1998). A Role for Superadiabatic Convection in Low Mass Structures?, *in* R. Rebolo, E. L. Martin, & M. R. Zapatero Osorio (ed.), *Brown Dwarfs and Extrasolar Planets*, Vol. 134 of *Astronomical Society of the Pacific Conference Series*, pp. 442–+.

Duchêne, G. (2008). High-angular resolution imaging of disks and planets, *NewAR* 52: 117–144.

Dupuy, T. J., Liu, M. C. & Ireland, M. J. (2009). Dynamical Mass of the Substellar Benchmark Binary HD 130948BC, *ApJ* 692: 729–752.

Faherty, J. K., Burgasser, A. J., West, A. A., Bochanski, J. J., Cruz, K. L., Shara, M. M. & Walter, F. M. (2010). The Brown Dwarf Kinematics Project. II. Details on Nine Wide Common Proper Motion Very Low Mass Companions to Nearby Stars, *AJ* 139: 176–194.

Freistetter, F., Krivov, A. V. & Löhne, T. (2007). Planets of β Pictoris revisited, *A&A* 466: 389–393.

Goldman, B., Marsat, S., Henning, T., Clemens, C. & Greiner, J. (2010). A new benchmark T8-9 brown dwarf and a couple of new mid-T dwarfs from the UKIDSS DR5+ LAS, *MNRAS* 405: 1140–1152.

Grether, D. & Lineweaver, C. H. (2006). How Dry is the Brown Dwarf Desert? Quantifying the Relative Number of Planets, Brown Dwarfs, and Stellar Companions around Nearby Sun-like Stars, *ApJ* 640: 1051–1062.

Guenther, E. W., Neuhäuser, R., Huélamo, N., Brandner, W. & Alves, J. (2001). Infrared spectrum and proper motion of the brown dwarf companion of HR 7329 in Tucanae, *A&A* 365: 514–518.

Hatzes, A. P., Cochran, W. D., McArthur, B., Baliunas, S. L., Walker, G. A. H., Campbell, B., Irwin, A. W., Yang, S., Kürster, M., Endl, M., Els, S., Butler, R. P. & Marcy, G. W. (2000). Evidence for a Long-Period Planet Orbiting ε Eridani, *ApJL* 544: L145–L148.

Ireland, M. J., Kraus, A., Martinache, F., Law, N. & Hillenbrand, L. A. (2011). Two Wide Planetary-mass Companions to Solar-type Stars in Upper Scorpius, *ApJ* 726: 113–+.

Itoh, Y., Hayashi, M., Tamura, M., Tsuji, T., Oasa, Y., Fukagawa, M., Hayashi, S. S., Naoi, T., Ishii, M., Mayama, S., Morino, J.-i., Yamashita, T., Pyo, T.-S., Nishikawa, T., Usuda, T.,

Murakawa, K., Suto, H., Oya, S., Takato, N., Ando, H., Miyama, S. M., Kobayashi, N. & Kaifu, N. (2005). A Young Brown Dwarf Companion to DH Tauri, *ApJ* 620: 984–993.

Janson, M., Bergfors, C., Goto, M., Brandner, W. & Lafrenière, D. (2010). Spatially Resolved Spectroscopy of the Exoplanet HR 8799 c, *ApJL* 710: L35–L38.

Janson, M., Brandner, W., Henning, T., Lenzen, R., McArthur, B., Benedict, G. F., Reffert, S., Nielsen, E., Close, L., Biller, B., Kellner, S., Günther, E., Hatzes, A., Masciadri, E., Geissler, K. & Hartung, M. (2007). NACO-SDI Direct Imaging Search for the Exoplanet ϵ Eri b, *AJ* 133: 2442–2456.

Janson, M., Brandner, W., Henning, T. & Zinnecker, H. (2006). Early ComeOn+ adaptive optics observation of GQ Lupi and its substellar companion, *A&A* 453: 609–614.

Jayawardhana, R. & Ivanov, V. D. (2006). Discovery of a Young Planetary-Mass Binary, *Science* 313: 1279–1281.

Kalas, P., Graham, J. R., Chiang, E., Fitzgerald, M. P., Clampin, M., Kite, E. S., Stapelfeldt, K., Marois, C. & Krist, J. (2008). Optical Images of an Exosolar Planet 25 Light-Years from Earth, *Science* 322: 1345–.

Konopacky, Q. M., Ghez, A. M., Duchêne, G., McCabe, C. & Macintosh, B. A. (2007). Measuring the Mass of a Pre-Main-Sequence Binary Star through the Orbit of TWA 5A, *AJ* 133: 2008–2014.

Kuzuhara, M., Tamura, M., Ishii, M., Kudo, T., Nishiyama, S. & Kandori, R. (2011). The Widest-separation Substellar Companion Candidate to a Binary T Tauri Star, *AJ* 141: 119–+.

Lacour, S., Tuthill, P., Amico, P., Ireland, M., Ehrenreich, D., Huelamo, N. & Lagrange, A.-M. (2011). Sparse aperture masking at the VLT. I. Faint companion detection limits for the two debris disk stars HD 92945 and HD 141569, *A&A* 532: A72+.

Lafrenière, D., Doyon, R., Nadeau, D., Artigau, É., Marois, C. & Beaulieu, M. (2007). Improving the Speckle Noise Attenuation of Simultaneous Spectral Differential Imaging with a Focal Plane Holographic Diffuser, *ApJ* 661: 1208–1217.

Lafrenière, D., Jayawardhana, R., Janson, M., Helling, C., Witte, S. & Hauschildt, P. (2011). Discovery of an 23 MJup Brown Dwarf Orbiting 700 AU from the Massive Star HIP 78530 in Upper Scorpius, *ApJ* 730: 42–+.

Lafrenière, D., Jayawardhana, R. & van Kerkwijk, M. H. (2008). Direct Imaging and Spectroscopy of a Planetary-Mass Candidate Companion to a Young Solar Analog, *ApJL* 689: L153–L156.

Lafrenière, D., Jayawardhana, R. & van Kerkwijk, M. H. (2010). The Directly Imaged Planet Around the Young Solar Analog 1RXS J160929.1 - 210524: Confirmation of Common Proper Motion, Temperature, and Mass, *ApJ* 719: 497–504.

Lafrenière, D., Marois, C., Doyon, R., Nadeau, D. & Artigau, É. (2007). A New Algorithm for Point-Spread Function Subtraction in High-Contrast Imaging: A Demonstration with Angular Differential Imaging, *ApJ* 660: 770–780.

Lagrange, A.-M., Bonnefoy, M., Chauvin, G., Apai, D., Ehrenreich, D., Boccaletti, A., Gratadour, D., Rouan, D., Mouillet, D., Lacour, S. & Kasper, M. (2010). A Giant Planet Imaged in the Disk of the Young Star β Pictoris, *Science* 329: 57–.

Lagrange, A.-M., Gratadour, D., Chauvin, G., Fusco, T., Ehrenreich, D., Mouillet, D., Rousset, G., Rouan, D., Allard, F., Gendron, É., Charton, J., Mugnier, L., Rabou, P., Montri, J. & Lacombe, F. (2009). A probable giant planet imaged in the β Pictoris disk. VLT/NaCo deep L'-band imaging, *A&A* 493: L21–L25.

Latham, D. W., Stefanik, R. P., Mazeh, T., Mayor, M. & Burki, G. (1989). The unseen companion of HD114762 - A probable brown dwarf, *Nature* 339: 38–40.

Liu, M. C., Delorme, P., Dupuy, T. J., Bowler, B. P., Albert, L., Artigau, E., Reyle, C., Forveille, T. & Delfosse, X. (2011). CFBDSIR J1458+1013B: A Very Cold (>T10) Brown Dwarf in a Binary System, *ArXiv e-prints* .

Lowrance, P. J., McCarthy, C., Becklin, E. E., Zuckerman, B., Schneider, G., Webb, R. A., Hines, D. C., Kirkpatrick, J. D., Koerner, D. W., Low, F., Meier, R., Rieke, M., Smith, B. A., Terrile, R. J. & Thompson, R. I. (1999). A Candidate Substellar Companion to CD -33 deg7795 (TWA 5), *ApJL* 512: L69–L72.

Lowrance, P. J., Schneider, G., Kirkpatrick, J. D., Becklin, E. E., Weinberger, A. J., Zuckerman, B., Plait, P., Malmuth, E. M., Heap, S. R., Schultz, A., Smith, B. A., Terrile, R. J. & Hines, D. C. (2000). A Candidate Substellar Companion to HR 7329, *ApJ* 541: 390–395.

Luhman, K. L., Burgasser, A. J. & Bochanski, J. J. (2011). Discovery of a Candidate for the Coolest Known Brown Dwarf, *ApJL* 730: L9+.

Luhman, K. L., Patten, B. M., Marengo, M., Schuster, M. T., Hora, J. L., Ellis, R. G., Stauffer, J. R., Sonnett, S. M., Winston, E., Gutermuth, R. A., Megeath, S. T., Backman, D. E., Henry, T. J., Werner, M. W. & Fazio, G. G. (2007). Discovery of Two T Dwarf Companions with the Spitzer Space Telescope, *ApJ* 654: 570–579.

Luhman, K. L., Wilson, J. C., Brandner, W., Skrutskie, M. F., Nelson, M. J., Smith, J. D., Peterson, D. E., Cushing, M. C. & Young, E. (2006). Discovery of a Young Substellar Companion in Chamaeleon, *ApJ* 649: 894–899.

Marois, C., Lafrenière, D., Doyon, R., Macintosh, B. & Nadeau, D. (2006). Angular Differential Imaging: A Powerful High-Contrast Imaging Technique, *ApJ* 641: 556–564.

Marois, C., Macintosh, B. & Barman, T. (2007). GQ Lup B Visible and Near-Infrared Photometric Analysis, *ApJL* 654: L151–L154.

Marois, C., Macintosh, B., Barman, T., Zuckerman, B., Song, I., Patience, J., Lafrenière, D. & Doyon, R. (2008). Direct Imaging of Multiple Planets Orbiting the Star HR 8799, *Science* 322: 1348–.

Marois, C., Zuckerman, B., Konopacky, Q. M., Macintosh, B. & Barman, T. (2010). Images of a fourth planet orbiting HR 8799, *Nature* 468: 1080–1083.

Mason, B. D., Wycoff, G. L., Hartkopf, W. I., Douglass, G. G. & Worley, C. E. (2001). The 2001 US Naval Observatory Double Star CD-ROM. I. The Washington Double Star Catalog, *AJ* 122: 3466–3471.

Mayor, M. & Queloz, D. (1995). A Jupiter-mass companion to a solar-type star, *Nature* 378: 355–359.

McElwain, M. W., Metchev, S. A., Larkin, J. E., Barczys, M., Iserlohe, C., Krabbe, A., Quirrenbach, A., Weiss, J. & Wright, S. A. (2007). First High-Contrast Science with an Integral Field Spectrograph: The Substellar Companion to GQ Lupi, *ApJ* 656: 505–514.

Metchev, S. A. & Hillenbrand, L. A. (2006). HD 203030B: An Unusually Cool Young Substellar Companion near the L/T Transition, *ApJ* 651: 1166–1176.

Metchev, S. A. & Hillenbrand, L. A. (2009). The Palomar/Keck Adaptive Optics Survey of Young Solar Analogs: Evidence for a Universal Companion Mass Function, *ApJS* 181: 62–109.

Metchev, S., Marois, C. & Zuckerman, B. (2009). Pre-Discovery 2007 Image of the HR 8799 Planetary System, *ApJL* 705: L204–L207.

Mohanty, S., Jayawardhana, R., Huélamo, N. & Mamajek, E. (2007). The Planetary Mass Companion 2MASS 1207-3932B: Temperature, Mass, and Evidence for an Edge-on Disk, *ApJ* 657: 1064–1091.

Mugrauer, M., Neuhaeuser, R., Guenther, E. & Mazeh, T. (2005). The multiplicity of exoplanet host stars., *Astronomische Nachrichten* 326: 629–630.

Mugrauer, M., Seifahrt, A., Neuhäuser, R. & Mazeh, T. (2006). HD3651B: the first directly imaged brown dwarf companion of an exoplanet host star, *MNRAS* 373: L31–L35.

Mugrauer, M., Vogt, N., Neuhäuser, R. & Schmidt, T. O. B. (2010). Direct detection of a substellar companion to the young nearby star PZ Telescopii, *A&A* 523: L1+.

Nakajima, T., Oppenheimer, B. R., Kulkarni, S. R., Golimowski, D. A., Matthews, K. & Durrance, S. T. (1995). Discovery of a cool brown dwarf, *Nature* 378: 463–465.

Neuhäuser, R. (2008). Homogeneous Comparison of Directly Detected Planet Candidates: GQ Lup, 2M1207, AB Pic, *in* S. Hubrig, M. Petr-Gotzens, & A. Tokovinin (ed.), *Multiple Stars Across the H-R Diagram*, pp. 183–+.

Neuhäuser, R., Brandner, W., Eckart, A., Guenther, E., Alves, J., Ott, T., Huélamo, N. & Fernández, M. (2000). On the possibility of ground-based direct imaging detection of extra-solar planets: the case of TWA-7, *A&A* 354: L9–L12.

Neuhäuser, R., Ginski, C., Schmidt, T. O. B. & Mugrauer, M. (2011). Further deep imaging of HR 7329 A (η Tel A) and its brown dwarf companion B, *MNRAS* pp. 1135–+.

Neuhäuser, R., Guenther, E., Brandner, W., Húelamo, N., Ott, T., Alves, J., Cómeron, F., Cuby, J.-G. & Eckart, A. (2002). Direct Imaging and Spectroscopy of Substellar Companions Next to Young Nearby Stars in TWA, *in* J. F. Alves & M. J. McCaughrean (ed.), *The Origin of Stars and Planets: The VLT View*, pp. 383–+.

Neuhäuser, R. & Guenther, E. W. (2004). Infrared spectroscopy of a brown dwarf companion candidate near the young star GSC 08047-00232 in Horologium, *A&A* 420: 647–653.

Neuhäuser, R., Guenther, E. W., Alves, J., Huélamo, N., Ott, T. & Eckart, A. (2003). An infrared imaging search for low-mass companions to members of the young nearby β Pic and Tucana/Horologium associations, *Astronomische Nachrichten* 324: 535–542.

Neuhäuser, R., Guenther, E. W., Petr, M. G., Brandner, W., Huélamo, N. & Alves, J. (2000). Spectrum and proper motion of a brown dwarf companion of the T Tauri star CoD-33 7795, *A&A* 360: L39–L42.

Neuhäuser, R., Guenther, E. W., Wuchterl, G., Mugrauer, M., Bedalov, A. & Hauschildt, P. H. (2005). Evidence for a co-moving sub-stellar companion of GQ Lup, *A&A* 435: L13–L16.

Neuhäuser, R., Mugrauer, M., Seifahrt, A., Schmidt, T. O. B. & Vogt, N. (2008). Astrometric and photometric monitoring of GQ Lupi and its sub-stellar companion, *A&A* 484: 281–291.

Neuhäuser, R., Schmidt, T. O. B., Hambaryan, V. V. & Vogt, N. (2010). Orbital motion of the young brown dwarf companion TWA 5 B, *A&A* 516: A112+.

Neuhäuser, R., Schmidt, T. O. B., Seifahrt, A., Bedalov, A., Helling, C., Witte, S. & Hauschildt, P. (2009). Medium-resolution infrared integral field spectroscopy of the brown dwarf TWA 5 B, *in* E. Stempels (ed.), *American Institute of Physics Conference Series*, Vol. 1094 of *American Institute of Physics Conference Series*, pp. 844–847.

Oppenheimer, B. R. & Hinkley, S. (2009). High-Contrast Observations in Optical and Infrared Astronomy, *ARofA&A* 47: 253–289.

Oppenheimer, B. R., Kulkarni, S. R., Matthews, K. & Nakajima, T. (1995). Infrared Spectrum of the Cool Brown Dwarf Gl 229B, *Science* 270: 1478–1479.

Quanz, S. P., Meyer, M. R., Kenworthy, M. A., Girard, J. H. V., Kasper, M., Lagrange, A.-M., Apai, D., Boccaletti, A., Bonnefoy, M., Chauvin, G., Hinz, P. M. & Lenzen, R. (2010). First Results from Very Large Telescope NACO Apodizing Phase Plate: 4 μm Images of The Exoplanet β Pictoris b, *ApJL* 722: L49–L53.

Rebolo, R., Zapatero Osorio, M. R., Madruga, S., Bejar, V. J. S., Arribas, S. & Licandro, J. (1998). Discovery of a Low-Mass Brown Dwarf Companion of the Young Nearby Star G 196-3, *Science* 282: 1309–+.

Reid, I. N. & Walkowicz, L. M. (2006). LP 261-75/2MASSW J09510549+3558021: A Young, Wide M4.5/L6 Binary, *PASP* 118: 671–677.

Reidemeister, M., Krivov, A. V., Schmidt, T. O. B., Fiedler, S., Müller, S., Löhne, T. & Neuhäuser, R. (2009). A possible architecture of the planetary system HR 8799, *A&A* 503: 247–258.

Rodriguez, D. R., Zuckerman, B., Melis, C. & Song, I. (2011). The Ultra Cool Brown Dwarf Companion of WD 0806-661B: Age, Mass, and Formation Mechanism, *ApJL* 732: L29+.

Sahlmann, J., Segransan, D., Queloz, D. & Udry, S. (2010). A possible dividing line between massive planets and brown-dwarf companions, *ArXiv e-prints* .

Schmidt, T. O. B., Neuhäuser, R. & Seifahrt, A. (2009). Homogeneous Comparison of Planet Candidates Imaged Directly Until 2008, *in* T. Usuda, M. Tamura, & M. Ishii (ed.), *American Institute of Physics Conference Series*, Vol. 1158 of *American Institute of Physics Conference Series*, pp. 231–234.

Schmidt, T. O. B., Neuhäuser, R., Seifahrt, A., Vogt, N., Bedalov, A., Helling, C., Witte, S. & Hauschildt, P. H. (2008). Direct evidence of a sub-stellar companion around CT Chamaeleontis, *A&A* 491: 311–320.

Schneider, J., Dedieu, C., Le Sidaner, P., Savalle, R. & Zolotukhin, I. (2011). Defining and cataloging exoplanets: the exoplanet.eu database, *A&A* 532: A79+.

Scholz, R.-D. (2010). Hip 63510C, Hip 73786B, and nine new isolated high proper motion T dwarf candidates from UKIDSS DR6 and SDSS DR7, *A&A* 515: A92+.

Seifahrt, A., Neuhäuser, R. & Hauschildt, P. H. (2007). Near-infrared integral-field spectroscopy of the companion to GQ Lupi, *A&A* 463: 309–313.

Stassun, K. G., Mathieu, R. D. & Valenti, J. A. (2006). Discovery of two young brown dwarfs in an eclipsing binary system, *Nature* 440: 311–314.

Stassun, K. G., Mathieu, R. D. & Valenti, J. A. (2007). A Surprising Reversal of Temperatures in the Brown Dwarf Eclipsing Binary 2MASS J05352184-0546085, *ApJ* 664: 1154–1166.

Thalmann, C., Carson, J., Janson, M., Goto, M., McElwain, M., Egner, S., Feldt, M., Hashimoto, J., Hayano, Y., Henning, T., Hodapp, K. W., Kandori, R., Klahr, H., Kudo, T., Kusakabe, N., Mordasini, C., Morino, J.-I., Suto, H., Suzuki, R. & Tamura, M. (2009). Discovery of the Coldest Imaged Companion of a Sun-like Star, *ApJL* 707: L123–L127.

Todorov, K., Luhman, K. L. & McLeod, K. K. (2010). Discovery of a Planetary-mass Companion to a Brown Dwarf in Taurus, *ApJL* 714: L84–L88.

Udry, S. (2010). Detection and characterization of exoplanets: from gaseous giants to super-Earths, *In the Spirit of Lyot 2010*.

Wahhaj, Z., Liu, M. C., Biller, B. A., Clarke, F., Nielsen, E. L., Close, L. M., Hayward, T. L., Mamajek, E. E., Cushing, M., Dupuy, T., Tecza, M., Thatte, N., Chun, M., Ftaclas, C., Hartung, M., Reid, I. N., Shkolnik, E. L., Alencar, S. H. P., Artymowicz, P., Boss, A., de Gouveia Dal Pino, E., Gregorio-Hetem, J., Ida, S., Kuchner, M., Lin, D. N. C. & Toomey, D. W. (2011). The Gemini NICI Planet-finding Campaign: Discovery of

a Substellar L Dwarf Companion to the Nearby Young M Dwarf CD-35 2722, *ApJ*
729: 139–+.

Webb, R. A., Zuckerman, B., Platais, I., Patience, J., White, R. J., Schwartz, M. J. & McCarthy, C.
(1999). Discovery of Seven T Tauri Stars and a Brown Dwarf Candidatein the Nearby
TW Hydrae Association, *ApJL* 512: L63–L67.

White, R. J., Ghez, A. M., Reid, I. N. & Schultz, G. (1999). A Test of Pre-Main-Sequence
Evolutionary Models across the Stellar/Substellar Boundary Based on Spectra of the
Young Quadruple GG Tauri, *ApJ* 520: 811–821.

Woitas, J., Leinert, C. & Köhler, R. (2001). Mass ratios of the components in T Tauri binary
systems and implications for multiple star formation, *A&A* 376: 982–996.

Wolszczan, A. & Frail, D. A. (1992). A planetary system around the millisecond pulsar
PSR1257 + 12, *Nature* 355: 145–147.

Wright, J. T., Fakhouri, O., Marcy, G. W., Han, E., Feng, Y., Johnson, J. A., Howard, A. W.,
Fischer, D. A., Valenti, J. A., Anderson, J. & Piskunov, N. (2011). The Exoplanet Orbit
Database, *PASP* 123: 412–422.

Zacharias, N., Monet, D. G., Levine, S. E., Urban, S. E., Gaume, R. & Wycoff, G. L. (2005).
NOMAD Catalog (Zacharias+ 2005), *VizieR Online Data Catalog* 1297: 0–+.

Zapatero Osorio, M. R., Rebolo, R., Bihain, G., Béjar, V. J. S., Caballero, J. A. & Álvarez, C.
(2010). Infrared and Kinematic Properties of the Substellar Object G 196-3 B, *ApJ*
715: 1408–1418.
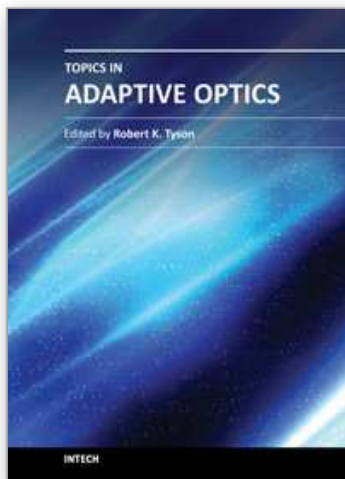
Advances in adaptive optics technology and applications move forward at a rapid pace. The basic idea of wavefront compensation in real-time has been around since the mid 1970s. The first widely used application of adaptive optics was for compensating atmospheric turbulence effects in astronomical imaging and laser beam propagation. While some topics have been researched and reported for years, even decades, new applications and advances in the supporting technologies occur almost daily. This book brings together 11 original chapters related to adaptive optics, written by an international group of invited authors. Topics include atmospheric turbulence characterization, astronomy with large telescopes, image post-processing, high power laser distortion compensation, adaptive optics and the human eye, wavefront sensors, and deformable mirrors.

How to reference

In order to correctly reference this scholarly work, feel free to copy and paste the following:

INTECH
open science | open minds